Full length article

Adverse (geno)toxic effects of bisphenol A and its analogues in hepatic 3D cell model

Marta Sendra [a,b,1], Martina Štampar [c,1], Katarina Fras [c], Beatriz Novoa [d], Antonio Figueras [d], Bojana Žegura [c,e,*]

[a] *Department of Biotechnology and Food Science, Faculty of Sciences, University of Burgos, Plaza Misael Bañuelos, 09001 Burgos, Spain*
[b] *International Research Center in Critical Raw Materials-ICCRAM, Universidad de Burgos, Plaza Misael Bañuelos s/n, 09001 Burgos, Spain*
[c] *National Institute of Biology, Department of Genetic Toxicology and Cancer Biology, 1000 Ljubljana, Slovenia*
[d] *Immunology and Genomics Group, Instituto de Investigaciones Marinas (IIM), Consejo Superior de Investigaciones Científicas (CSIC), Vigo, Spain*
[e] *Jozef Stefan International Postgraduate School, 1000 Ljubljana, Slovenia*

ARTICLE INFO

ABSTRACT

Bisphenol A (BPA) is one of the most widely used and versatile chemical compounds in polymer additives and epoxy resins for manufacturing a range of products for human applications. It is known as endocrine disruptor, however, there is growing evidence that it is genotoxic. Because of its adverse effects, the European Union has restricted its use to protect human health and the environment. As a result, the industry has begun developing BPA analogues, but there are not yet sufficient toxicity data to claim that they are safe. We investigated the adverse toxic effects of BPA and its analogues (BPS, BPAP, BPAF, BPFL, and BPC) with emphasis on their cytotoxic and genotoxic activities after short (24-h) and prolonged (96-h) exposure in *in vitro* hepatic three-dimensional cell model developed from HepG2 cells. The results showed that BPFL and BPC (formed by an additional ring system) were the most cytotoxic analogues that affected cell viability, spheroid surface area and morphology, cell proliferation, and apoptotic cell death. BPA, BPAP, and BPAF induced DNA double-strand break formation (γH2AX assay), whereas BPAF and BPC increased the percentage of p-H3-positive cells, indicating their aneugenic activity. All BPs induced DNA single-strand break formation (comet assay), with BPAP ($\geq$0.1 μM) being the most effective and BPA and BPC the least effective ($\geq$1 μM) under conditions applied. The results indicate that not all of the analogues studied are safer alternatives to BPA and thus more in-depth research is urgently needed to adequately evaluate the risks of BPA analogues and assess their safety for humans.

1. Introduction

In recent decades, there has been a significant increase in the number of chemical additives used in industry to improve the physical and chemical properties of products for human use (Thomas, 2016). Bisphenols (BPs) are synthetic chemicals used in a wide range of industrial applications for the manufacture of epoxy resins, polycarbonate plastics, and other polymers used to manufacture a wide range of daily products, including media, construction, optics, automotive, electrical and electronics, medical, food packaging, housewares and appliances, interior surface coatings, metal beverage cans, dental sealants, and thermal paper products (Ballesteros-Gómez et al., 2014). The widespread use of BPA and its leaching from consumer products has resulted in its ubiquity in the environment. This leads to chronic exposure through diet (food and water) and other means (inhalation, absorption), which is of great concern as many studies report that BPA causes adverse effects on human health and the environment (Masoner et al., 2014; Kawagoshi et al., 2003; Coors et al., 2003). It is known as an endocrine-disrupting chemical (EDC) (Cantonwine et al., 2013; Wisniewski et al., 2015; Zhou et al., 2017), and an increasing number of studies have reported its genotoxic properties (Usman and Ahmad, 2016; Pradesh et al., 2018; Seachrist et al., 2016). It can cause reproductive, metabolic (metabolic dysfunctions, diabetes, obesity), immunological, cardiovascular, renal, respiratory, and tumour problems

---

(Rezg et al., 2014; Rochester, 2013; Sendra et al., 2020; Vandenberg et al., 2012) and impairs cognitive and behavioural development (Galloway et al., 2018), which has raised questions about its safety. Due to its hazardous characteristics, the use of BPA has been restricted in the European Union in order to protect the environment and human health (Lucarini et al., 2020).

In 2012 and 2013, the U.S. Food and Drug Administration (FDA) revised its regulations to ban the use of BPA-containing polycarbonate resins in baby bottles and cups and the use of BPA-containing epoxy resins as coatings in the packaging of infant formula, respectively (FDA, 2014). Further on, in 2017 the European Chemical Agency (ECHA) included BPA to the Candidate List of Substances of Very High Concern (SVHC), and the authorities have been encouraging the replacement of BPA with presumably safer analogues. In the same year, the European Food Safety Authority (EFSA) proposed a provisional daily intake limit for BPA of 4 g/Kg body weight per day (EFSA, 2015), and in 2018, the EU Regulation (No. 2018/213) lowered the limit for migration of BPA from food packaging materials into food from 0.6 mg·Kg^{-1} to 0.05 mg·Kg^{-1}. Moreover, the migration of BPA into any baby food or infant formula has been prohibited (Commission, 2018). Since 2018, the EU requires that products containing BPA are classified and labelled as toxic for reproduction (den Braver-Sewradj et al., 2020). In addition, the use of BPA in the thermal paper is restricted from 2020 by EU Regulation 2016/2235 and REACH (Registration, Evaluation, Authorization, and Restriction of Chemicals) (https://echa.europa.eu/).

All of these restrictions on the use of BPA in consumer products due to its harmful effects have prompted the industry to develop more than 200 BPA analogues, presumably as safer alternatives, and global industrial production of BPA analogues is expected to increase even further in the near future (Lucarini et al., 2020; den Braver-Sewradj et al., 2020; Pelch et al., 2019; Russo et al., 2019). The widespread use of these products has inevitably led to contamination of outdoor and indoor environments and food, which in turn affects human health. To date, most BPA analogues have not been regulated or included in legislation (Lucarini et al., 2020), even though many of them already appear to be harmful to humans. In the last two decades, much attention has been paid in particular to the toxicity of BPA, while few data are available on BPA analogues, although they are threatening to become one of the most important environmental pollutants (Liu et al., 2021), at concentrations sometimes higher than BPA (Pelch et al., 2019). Nevertheless, the presence and internal exposure risks of BPA analogues in the general population remain poorly understood (Pelch et al., 2019; Jin et al., 2018; Chen et al., 2016). BPA analogues can be divided into two main groups: unsubstituted (e.g., BPAP, BPE, BPF, and BPB) and substituted phenol rings (e.g., BPC and BPPH). In the group of unsubstituted phenol rings, the analogues are classified as methyl or ethyl groups at carbon bridge, ring system at carbon bridge, or other functional groups at carbon bridge. The group of substituted phenol rings is divided into methyl groups as substituents and ring systems as substituents (Zühlke et al., 2020) (Table 1).

Bisphenol-S [4,4′-sulfonyldiphenol (BPS)] as one of the first substitutes for BPA is commonly used in canned foodstuffs, epoxy glues, food cartons, thermal receipt papers, luggage tags, flyers, newspapers etc. (Liao et al., 2012). Literature data suggest that it may act as an EDC similar to BPA and therefore also needs to be subjected to the restrictions on BPA at REACH (EU, 2006). ECHA is currently reviewing BPS for its endocrine-disrupting properties (ECHA, 2020), however, it is still approved for use in food contact materials under Regulation No 10/2011. Bisphenol-AP [4,4′-(1-phenylethylidene)bisphenol (BPAP)] and bisphenol-FL [9,9-bis(4-hydroxyphenyl)fluorene (BPFL)] are widely used for the synthesis of polyester polymers such as epoxy resins, polycarbonates, polyesters, polyurethanes, polyethers, and polyacrylates (Liu et al., 2008; Dai et al., 2009), especially as indispensable plasticizers and flame retardants (Zhang et al., 2013). Although BPAP is a poorly studied BPA analogue, it has been confirmed as an EDC (Xiao et al., 2018). Bisphenol-AF [4,4′-(hexafluoroisopropylidene)diphenol (BPAF)] is widely used in the industry as O-rings, seals, and gaskets due to its thermal stability, chemical resistance, and resistance to compression set (Choi and Lee, 2017). ECHA has included BPAF in the list of substances of concern because data show that it is toxic for reproduction (ECHA,

Table 1
Physical and chemical characteristics of BPA and its analogues (BPS, BPAF, BPAP, BPFL and BPC) selected in this work.

Classification according to phenol ring	Functional groups at carbon bridge	Name	Abbreviation	Synonym	CAS N°	Chemical structure	Formula	MW (g·mol^{-1})
Unsubstituted phenol ring	Methyl or ethyl groups at carbon bridge	BPA	Bisphenol A	2,2-bis(4-hydroxyphenyl) propane	080–05–7		C15H16O2	228.29
	Other functional groups at the carbon bridge	BPS	Bisphenol S	4,4′-Sulfonyldiphenol	080–09–1		C12H10O4S	250.27
		BPAF	Bisphenol AF	4,4′-(hexafluoroisopropylidene) diphenol	1478–61-1		C15H10F6O2	336.23
	Ring system at carbon bridge	BPAP	Bisphenol AP	4,4′-(1-Phenylethylidene) bisphenol	1571–75-1		CH3C(C6H5)(C6H4OH)2	290.36
		BPFL	Bisphenol FL	9,9-Bis(4-hydroxyphenyl) fluorene	3236–71-3		C25H18O2	350.41
Substituted phenol ring	Methyl groups as substituents	BPC	Bisphenol C	4,4′-Isopropylidenedi-o-cresol	79–97-0		(CH3)2C[C6H3(CH3)OH]2	256.34

2019). Bisphenol C [4,4′-isopropylidenedi-o-cresol (BPC)] is one of the most versatile BPs used in a wide variety of products and articles such as furniture, flooring, curtains, paper products, construction materials, toys, textiles, electronic devices, and food packaging and storage. Currently, BPC is being evaluated by ECHA under the Community Rolling Action Plan (CoRAP) for suspected reproductive toxicity and potential endocrine-disrupting properties (ECHA, 2021).

Although a growing number of studies show that many BPA analogues already used by industry are not only endocrine disruptors, but also have harmful genotoxic effects by inducing DNA strand breaks, affecting cell cycle, and cell proliferation, altering the expression of genes involved in DNA damage response and repair, and causing many other changes in cellular functions (Liao et al., 2012; Ikhlas et al., 2019; Kim et al., 2017; Shen et al., 2014; Fic et al., 2013; Hercog et al., 2019).

Here, we aimed to investigate the adverse toxic effects of BPA and its analogues, namely BPS, BPAP, BPAF, BPFL and BPC, with emphasis on their genotoxic activities due to ECHA recommendations and to unravel the underlying mechanisms of action. The analogues were selected based on their occurrence in foodstuffs (Caballero-Casero et al., 2016; Liao and Kannan, 2013), production volume (ECHA, 2021), occurrence in human samples (Chen et al., 2018) and structural diversity of their chemical formula. BPA and its analogues are known to be metabolised in organisms (Pritchett et al., 2002; Gramec Skledar and Peterlin Mašič, 2016; Štampar et al., 2020), therefore, in the present study we used an experimental model with metabolically competent human hepatocellular carcinoma (HepG2) cells to investigate the adverse effects of BPA and its analogues. Cells were grown in a three-dimensional (3D) shape called spheroids, as 3D cell models have recently been shown to better reflect *in vivo* conditions than traditional 2D cell models. Important advantages of culturing cells in 3D form include enhanced cell–cell and cell–matrix interactions and higher expression of liver-specific functions such as urea synthesis, albumin content, and expression of phase I and II enzymes, resulting in a more physiologically relevant model for human exposure (Štampar et al., 2022; Štampar et al., 2019; Conway et al., 2020).

In recent years, hepatic 3D cell models have been increasingly used as *in vitro* preclinical test systems due to their improved metabolic, structural, and physiological properties compared with traditional *in vitro* two-dimensional (2D) cell models (Conway et al., 2020; Elje et al., 2019; Elje et al., 2020; Llewellyn et al., 2020; Mandon et al., 2019; Pfuhler et al., 2020; Shah et al., 2020; Shah, 2018; Štampar et al., 2020; Bell et al., 2016). Such 3D cell models, unlike monolayer cultures, can be grown undisturbed for longer periods of time, and allow for prolonged exposure due to their greater stability, maintaining high cell viability and morphology for up to several weeks, making them a suitable model for chronic repeated dose studies (Bell et al., 2016; Bokhari et al., 2007; Eilenberger et al., 2019; Hughes, 2008; Shah et al., 2020; Štampar et al., 2020; Wrzesinski and Fey, 2015; Pfuhler et al., 2020). In our study, 3D models (spheroids) were exposed to BPs in the form of single compounds for 24 and 96-hours The effects of BPs and its analogues on spheroid growth was monitored with planimetry by light microscopy, while the cytotoxic effects were assessed by the MTS assay. Furthermore, a flow cytometric approach for simultaneous detection of specific lesions was used for investigating the cell cycle (Hoechst staining), cell proliferation (KI67 antibodies), mitotic cells (p-H3) and DNA double-strand breaks (γH2AX antibodies). In addition, flow cytometric analyses were applied for determination of spheroid cell death (necrosis/apoptosis) by staining with the PI/ Annexin-V. The induction of DNA single strand breaks was detected with the comet assay.

2. Materials and methods

2.1. Chemicals

A list of all reagents and chemicals is given in detail in the Supplementary Information (SI, Section SI-2).

2.2. Cell culture and formation of 3D spheroids

A human hepatocellular carcinoma cell line (HepG2) was purchased from the cell bank (ATCC-HB-8065™). The cells were grown in MEME media supplemented with FBS (10 %), NEAA, Na-pyruvate (0.1 g/mL), pen/strep (100 IU/mL), and ʟ-glutamine (2 mM) at 37 °C in 5 % CO_2 atmosphere. For the spheroid formation, the forced floating method explained in Štampar et al. (2019) was used. The spheroids with an initial density of 3.000 cells/spheroid were seeded onto 96-well plates and were grown for 3 days.

2.3. Treatment conditions

After 3 days of culture, the growth media was removed and the spheroids were exposed to the following bisphenols: BPA, BPS, BPAP, BPAF, BPFL and BPC as single compounds (BPs; Table 1) for 24-h and 96-h. For the 96-h exposure, the media was replaced after 48 h with fresh media containing the same concentration of BPs. In all experiments, solvent and appropriate positive controls (PC) were included.

2.4. Cytotoxic effects of bisphenols determined by MTS assay

The impact of the following BPs: BPA, BPS, BPAP, BPAF, BPFL and BPC on cell viability in spheroids after 24 and 96-hour exposure was determined by the tetrazolium-based assay (MTS). The spheroids were treated with 5, 10, 20, 40, 80 and 160 μM of BPs for 24-h and 2.5, 5, 10, 20, 40 and 80 μM of BPs for 96-h. The absorbance at 490 nm was measured using the spectrofluorimeter (Synergy MX, BioTek, USA). Etoposide (17 μM) served as a positive control (PC). Three independent biological replicates were performed and each time five spheroids per experimental point were measured. The difference between solvent control and treated groups was analysed by the One-way ANOVA with the post hoc multiple comparisons Dunnetts test using Sigma Plot software [$p < 0.05$ (*), $p < 0.001$ (**), $p < 0.0001$ (***) were considered statistically significant].

2.5. The measurements of surface area, shape and compactness of spheroids

The surface area (mm^2) and micrographs of at least 10 spheroids in each experiment performed in three independent biological replicates were recorded from day 3 - immediately before BPs treatment, and after 24- and 96- h of post-treatment. Micrographs were captured by the Ti Eclipse inverted microscope (Nikon, Japan) at 10x magnification equipped with a Nikon camera. For the evaluation of micrographs and planimetry, the ImageJ software was used. The graphical and statistical analysis was done with Sigma Plot software through a One-way ANOVA test with a Dunnett post hoc [$p < 0.05$ (*), $p < 0.001$ (**), $p < 0.0001$ (***) were considered statistically significant].

2.6. Flow cytometry analysis

2.6.1. Determination of spheroid cell death

Detection of cell death (apoptosis/ necrosis) induced by BPs was performed by flow cytometry as previously described by Lah at al. (Lah et al., 2021) with minor modifications. Subsequently, five spheroids per experimental point were collected, pooled and split by a combination of enzymatic digestion (5 mg/mL collagenase in MEME without supplements diluted with TryplE in the ratio 1:2) and mechanical degradation into a viable single-cell suspension as previously described by Štampar et al. (Štampar et al., 2020) with minor modification. Afterwards, the spheroids were disassembled into a single cell suspension by using 200 μL cut pipette tips. Subsequently, the cell viability was estimated by Trypan Blue (0.4 %) staining. Spheroids were treated with BPs for 24-h (0.1, 1, 10 and 40 μM) and 96-h (0.01, 0.1, 1 and 10 μM). Early/late apoptosis was determined by staining the cells with 1 mg/ml Annexin-V-

FITC and 1 g/ml PI (propidium iodide) solution for 15 min at room temperature in the dark. The measurements were done using a flow cytometer MACSQuant Analyzer 10 (Miltenyi Biotech, Germany) and the results were analysed by the FlowJo software V10 (New Jersey USA). In all experiments, solvent and positive controls were included. Staurosporine (2 µM) was used as a PC. The graphical and statistical analysis was done by One-way ANOVA with the post hoc multiple comparisons Dunnet́s test with Sigma Plot software [p < 0.05 (*), p < 0.001 (**), p < 0.0001 (***) were considered statistically significant].

2.6.2. Concurrent measurement of the cell proliferation, cell cycle, gamma-H2AX and histone-H3 positive cells by flow cytometry

After 24 and 96-h exposure to BPs, 30 spheroids were collected, pooled and split into the single-cell suspension as described above (Section Determination of DNA damage induced by BPs - Comet assay). Cells were then washed with 1x PBS and fixed with 4 % paraformaldehyde for 15 min at room temperature, followed by washing with PBS and permeabilization with 0.1 % Triton X-100. Fixed cells were washed and centrifuged at 1300 rpm for 10 min in cold PBS and labelled with anti-Ki-67-FITC, anti-H2AX pS139-APC, and anti-Histone H3 pS28-PE (1:50 diluted antibodies in 1 % BSA) for 30 min at room temperature, subsequently washed with 1x PBS and stained with Hoechst 33,258 dye (1:500 dilution in 0.1 % Triton X-100) for 20 min at room temperature as described by Hercog et al. (Hercog et al., 2019) and Štampar et al. (Štampar et al., 2022). FITC fluorescence signal was detected in the B1 channel (525/50 nm), Hoechst fluorescence signal was detected in the V1 channel (450/50 nm), APC fluorescence signal was detected in the R1 channel (655/73 nm) and PE fluorescence signal was detected in the B2 channel (585/40 nm). Rea-FITC, Rea-APC and Rea-H3 controls (Miltenyi Biotec, Germany) were used to avoid the non-specific antibody binding. Etoposide (1.7 µM) and Colchicine (0.1 µM) served as PC. The experiments were conducted in three biological replicates, where 20.000 single cells were recorded per experimental point. The data were analysed using the FlowJo software V10 (New Jersey USA) and graphically presented in the Sigma Plot. The statistical analysis of the frequency distributions of cells in the cell cycle (the percentage of cells in the G0/G1, S, and G2 phase) was performed by the multinomial logistic regression, and additional post estimation tests in Stata 15 (StataCorp LLC, USA). The statistical analysis of Ki67 and mitotic cells (H3 positive cells) was performed with the Sigma Plot program by the one-way ANOVA with Dunnett's multiple comparison test [*p < 0.05 was considered statistically significant], while the difference of H2AX positive cells among treated and control groups was tested using exported. csv values in the R software with the Mixed Effects Models (nlme) package by REML as described in Ramaiahgari et al. (Ramaiahgari et al., 2014), [*p < 0.05 was considered statistically significant].

2.7. Determination of DNA damage induced by BPs – Comet assay

Three-day-old spheroids were exposed to BPs for 24-h (1, 10 and 40 µM), and 96-h (0.1, 1 and 10 µM). Subsequently, five spheroids were collected, split into single-cell suspension (Štampar et al., 2020) as described above (Subsection 2.6.1 Determination of spheroid cell death), pelleted, and washed with 1 × PBS. The comet assay was performed on single-cell suspension according to Štampar et al. (Štampar et al., 2020), as described in MIRCA guidelines (Møller et al., 2020). Briefly, 30 µL of cell suspension was mixed with 70 µL of 1 % LMP agarose and added to the fully frosted slides that had been covered with a layer of 1 % NMP agarose. The slides were lysed (0.1 M EDTA, 2.5 M NaOH, pH 10, 0.01 M Tris and 1 % Triton X-100) for 1 h at 4 °C, unwound and electrophoresed (300 mM NaOH, 1 mM EDTA, pH 13) for 20 min at 25 V and 300 mA (0.5–1 V/cm). The slides were then neutralized (0.4 M Tris buffer; pH 7.5) for 15 min and the gels were stained with Gelred (Biotium, Fremont CA). Etoposide (17 µM) was used as a PC. The slides were evaluated with the fluorescence microscope (Eclipse 800, Nikon, Japan) equipped with a Basler camera and the comets were

analysed by Comet IV image analysis software from Perceptive Instruments (UK). Fifty randomly selected nuclei were analysed per experimental point, and experiments were repeated in three independent replicates. The results are presented as % of tail DNA. Statistical analysis was conducted with Sigma Plot software by two-way ANOVA post hoc multiple comparisons Dunnet́s test [p < 0.05 (*), p < 0.001 (**), p < 0.0001 (***) were considered statistically significant].

3. Results

### 3.1. The impact of BPA and its analogues on the viability of HepG2 cells in spheroids

The impact of BPA and its analogues (Table 1) on the viability of HepG2 cells in 3-day-old spheroids after subsequent 24 and 96-h exposure was determined with the MTS assay (Fig. 1). The results showed that studied BPs did not affect cell viability at concentrations applied (up to 160 and 80 µM, respectively), with the exception of BPFL and BPC. Spheroids exposed to BPFL at 160 µM for 24-h and 80 µM for 96-h showed a significant decrease in metabolic activity of approximately 38 % and 35 %, respectively, compared to solvent control (0.251 % DMSO). The analogue BPC significantly reduced cell viability at 80 µM after 96-h exposure for approximately 35 %, compared to solvent control (0.063 % DMSO). The positive control etoposide (17 µM) reduced the metabolic activity of HepG2 cells by approximately 29 % and 35 % after 24 and 96- h, respectively, compared to solvent control.

### 3.2. The impact of BPA and its analogues on the average surface area, shape and compactness of spheroids.

The surface area of 3-day old spheroids was monitored at three different time points: at time 0 (3-day old), which was immediately before the exposure to BPs and after subsequent 24 and 96-h exposure to six studied BPs at 2.5, 5, 10, 20, 40, 80 and 160 µM (Fig. 2 and Table S1). The results revealed no significant changes in the average surface area after 24-h exposure to BPs compared to the average surface area of solvent control. After 96-h of exposure, a slight however non-significant dose-dependent decrease in the average surface area was detected for BPA, BPS, BPAP and BPAF, while for BPFL and BPC, a significant 1.61- and 1.35-fold decrease, respectively, in the average surface area in comparison to solvent control was determined at 160 µM (Fig. 2A). Additionally, light microscopy analysis showed changes in the roundness, size, shape and compactness of the spheroids after 96-h of exposure to BPs compared to solvent control (Fig. 2B). BPA and BPS induced changes at 160 µM, while for BPAP, BPFL, BPAF and BPC, changes were observed ≥ 40 µM. Positive control etoposide (17 µM) significantly reduced the average spheroid surface area by 9.51 % in comparison to solvent control after 96-h of exposure.

3.3. The influence of BPA and its analogues on HepG2 cell death and apoptosis

The influence of BPs on HepG2 cell death trough apoptotic pathways was studied by analysing the percentage of early and late apoptotic cells, viable cells and necrotic cells using flow cytometry (Fig. 3A and 3B and Table S2). The number of early apoptotic cells (labelled with annexin-V-FITC) increased to approximately 15–20 % of total cells in BPS, BPAP, BPAF, BPFL and BPC at 40 µM after 24-h exposure. In the solvent control and BPA (40 µM), the percentage of early apoptotic cells accounted for approximately 3 % of total cells, (Fig. 3A). A significant increase in the amount of late apoptotic cells (annexin-V-FITC/PI stained) was observed after the exposure to all BPs except for BPAF. For all BPs, the amount of viable cells decreased in a dose-dependent manner, with the highest decrease determined for BPS and BPFL, where the percentage of viable cells at 40 µM accounted for 57 % and 58 % of the total cells, respectively. After 24-hour exposure of spheroids to BPA (40 µM), the
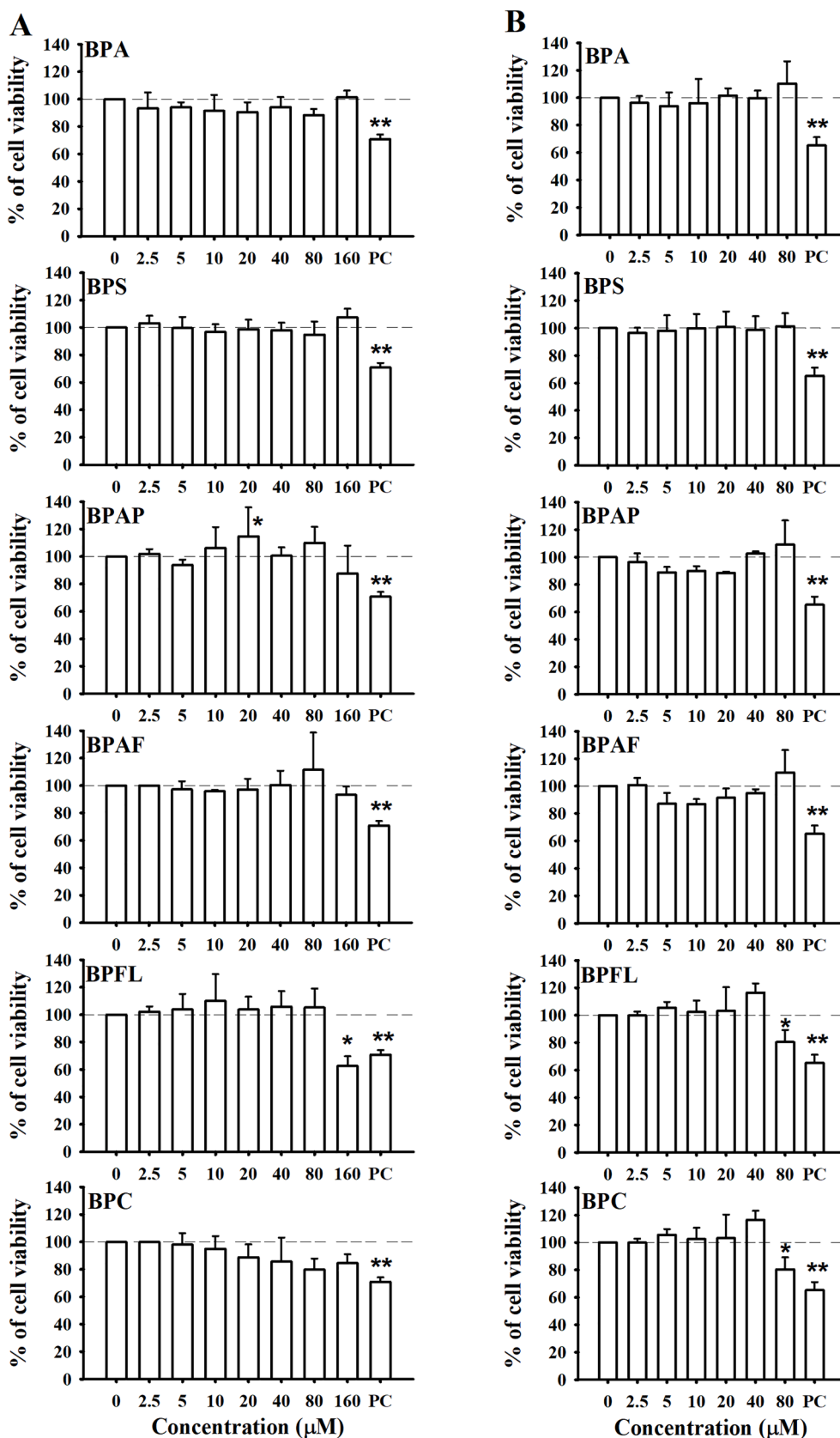
Fig. 1. Cell viability of HepG2 spheroids after 24 (A) and 96-h (B) of exposure to selected BPs assessed by MTS assay. Etoposide (17 μM) served as a positive control (PC). Results are presented as % of viable cells ± SD normalized to the solvent control (0). Statistical analysis was performed by the Two-way ANOVA with a Dunnett's post hoc test [p < 0.05 (*), p < 0.001 (**)].
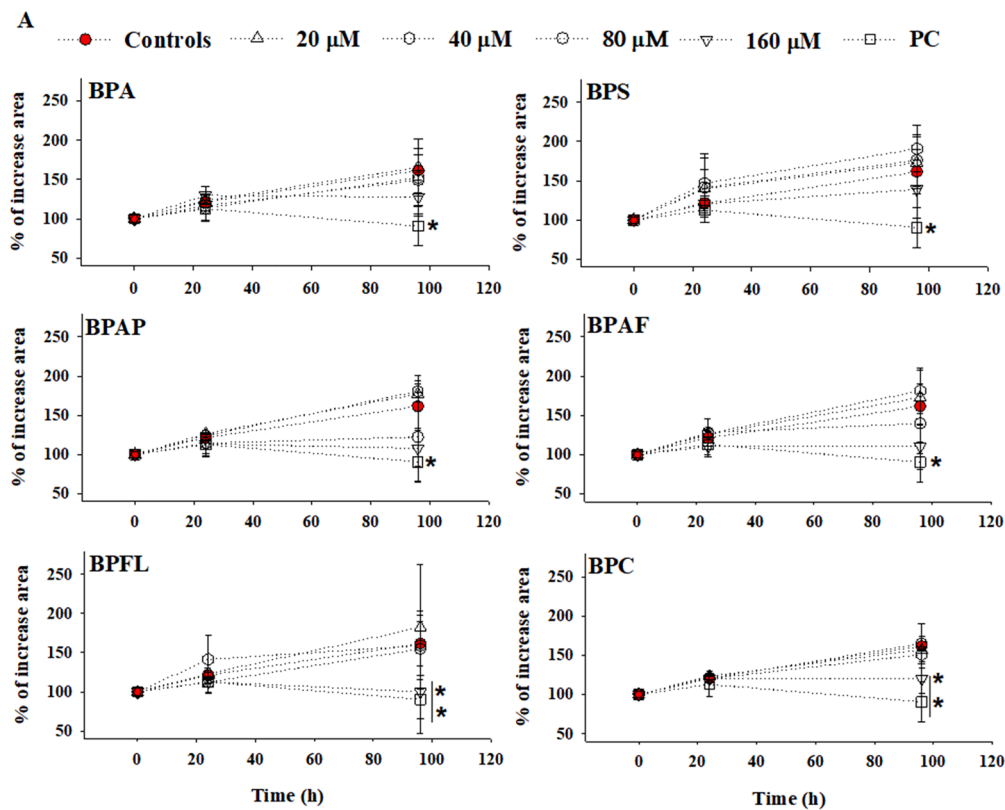
Fig. 2. Planimetry measurements of spheroids before treatment (72 h old) and after 24 and 96-h of treatment with selected BPs. A) Figures show the change in % of the average spheroid area compared to the average area of the 72-h old spheroid. B) Representative light microscopy showing changes in average surface area, compactness, and shape of 72-h-old spheroids exposed to BPs for 96-h. The growth of spheroids was monitored at 10x magnification using Ti Eclipse inverted microscope (Nikon). Etoposide (17 μM) served as a positive control (PC). Results are presented as mean ± SD (N = 10) of three biologically independent experiments. Statistical analysis was conducted in SigmaPlot.11 by the Two-ANOVA with a Dunnett's post hoc test [p < 0.05 (*)].
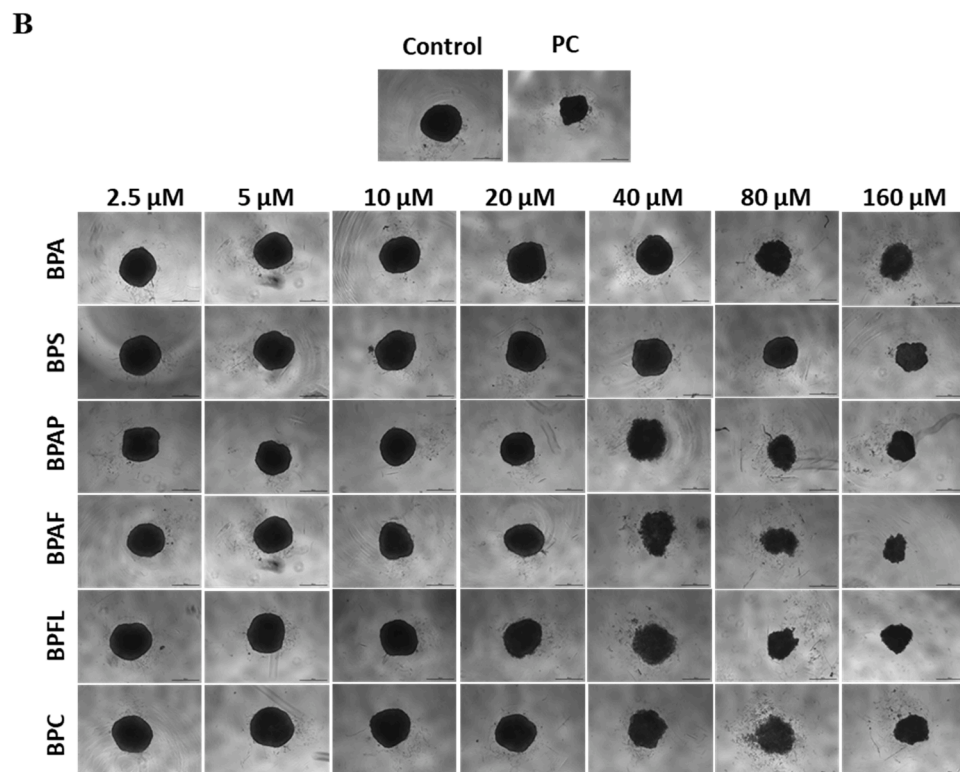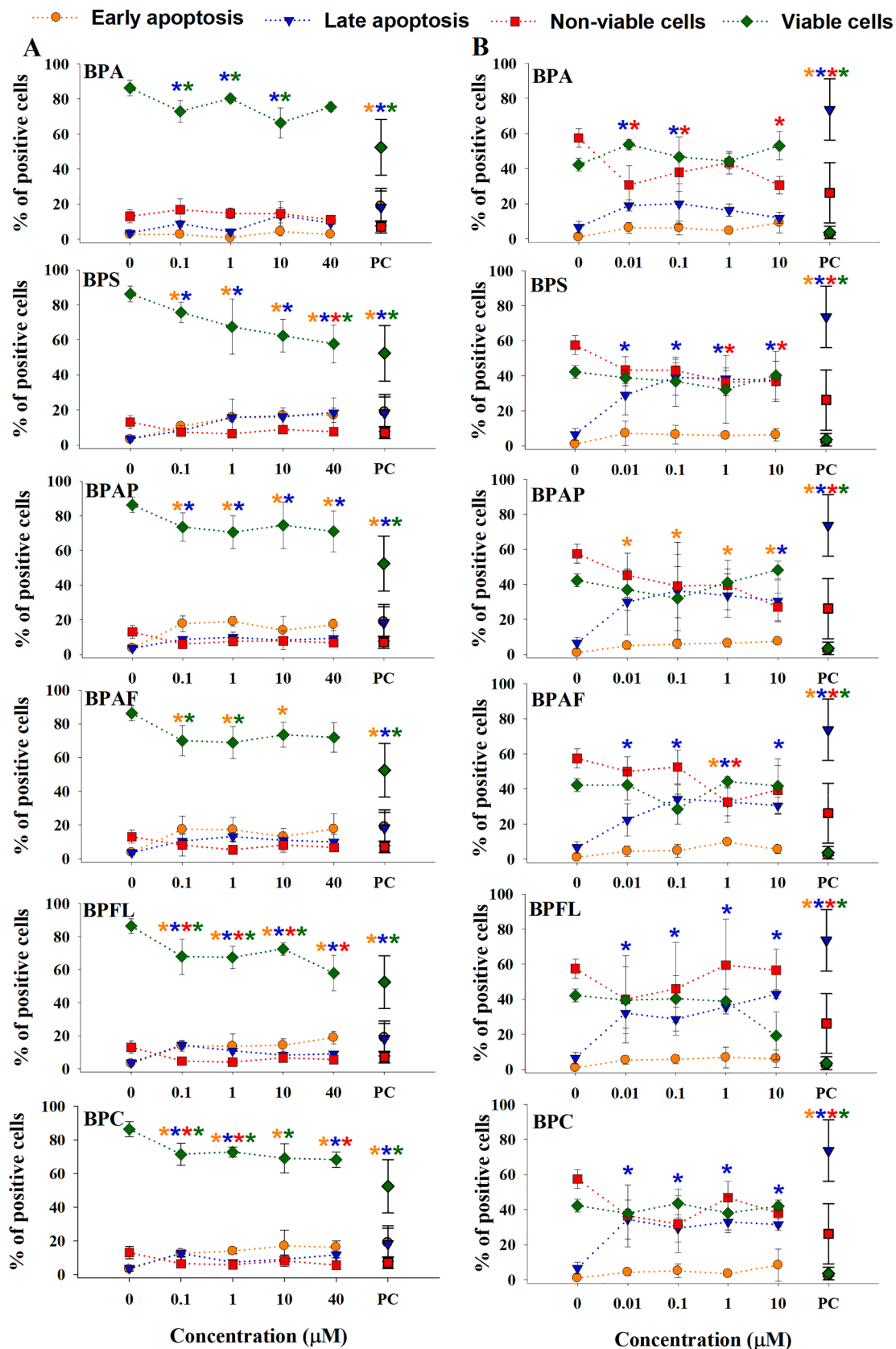
Fig. 3. Determination of cell death in HepG2 cells from spheroids exposed to selected BPs for 24 (A) and 96-h (B) by flow cytometry. Summary plots represent the percentage of early apoptotic, late apoptotic, non-viable and viable cells after treatment. Cells were labelled with Annexin V-FITC and propidium iodide (PI). Staurosporine (2 μM) served as a positive control (PC). Results are presented as mean + SD (N = 3) in SigmaPlot.11 and statistical analysis was performed by Two-way ANOVA with a Dunnett's post hoc test [p < 0.05 (*)]. The colour of the asterisks represents the significant difference in the response cited.

percentage of viable cells accounted for approximately 80 % of all cells, while in the solvent control group 90 % of cells were viable. Furthermore, a significant decrease in the amount of necrotic cells (PI stained) after 24-hour exposure of HepG2 spheroids to BPS, BPFL and BPC was measured, which was mostly due to an increase in the number of early and late apoptotic cells in the corresponding group.

After 96-h (Fig. 3B), the amount of early apoptotic cells was significantly elevated only after the exposure to BPAP (≥0.01 µM) and BPAF at 1 µM. The percentage of late apoptotic cells after exposure to all BPs increased dose-dependently reaching approximately 30–40 % of total cells at 10 µM, with the lowest increase, detected for BPA, approximately 18 % at 10 µM. On the other hand, the percentage of viable cells decreased significantly only after the exposure to BPFL (10 µM) and accounted for only 19 % of all cells. Interestingly the percentage of

viable cells was the highest after BPA exposure (53 % at 10 µM), while in the control group 42 % of all cells were viable. The amount of necrotic cells was the highest in the control group (approximately 57 %), while in BPs groups (at 10 µM) 30–57 % of cells were necrotic, with the highest values for BPFL (57 % of necrotic cells). The lowest percentage of necrotic cells was determined for BPA and BPAP, which at the same time had the highest percentage of viable cells.

Staurosporine, a well-known apoptogenic agent (Emanuelsson and Norlin, 2012), was used as a positive control. The results showed that staurosporine (2 µM) after 24-hours induced an increase in the number of early and late apoptotic cells, which accounted for 19 and 18 % of all cells, respectively. The percentages of necrotic and viable cells were approximately 7 and 52 %, respectively, of all cells. After 96-h, staurosporine induced an increase in the amount of early and late apoptotic
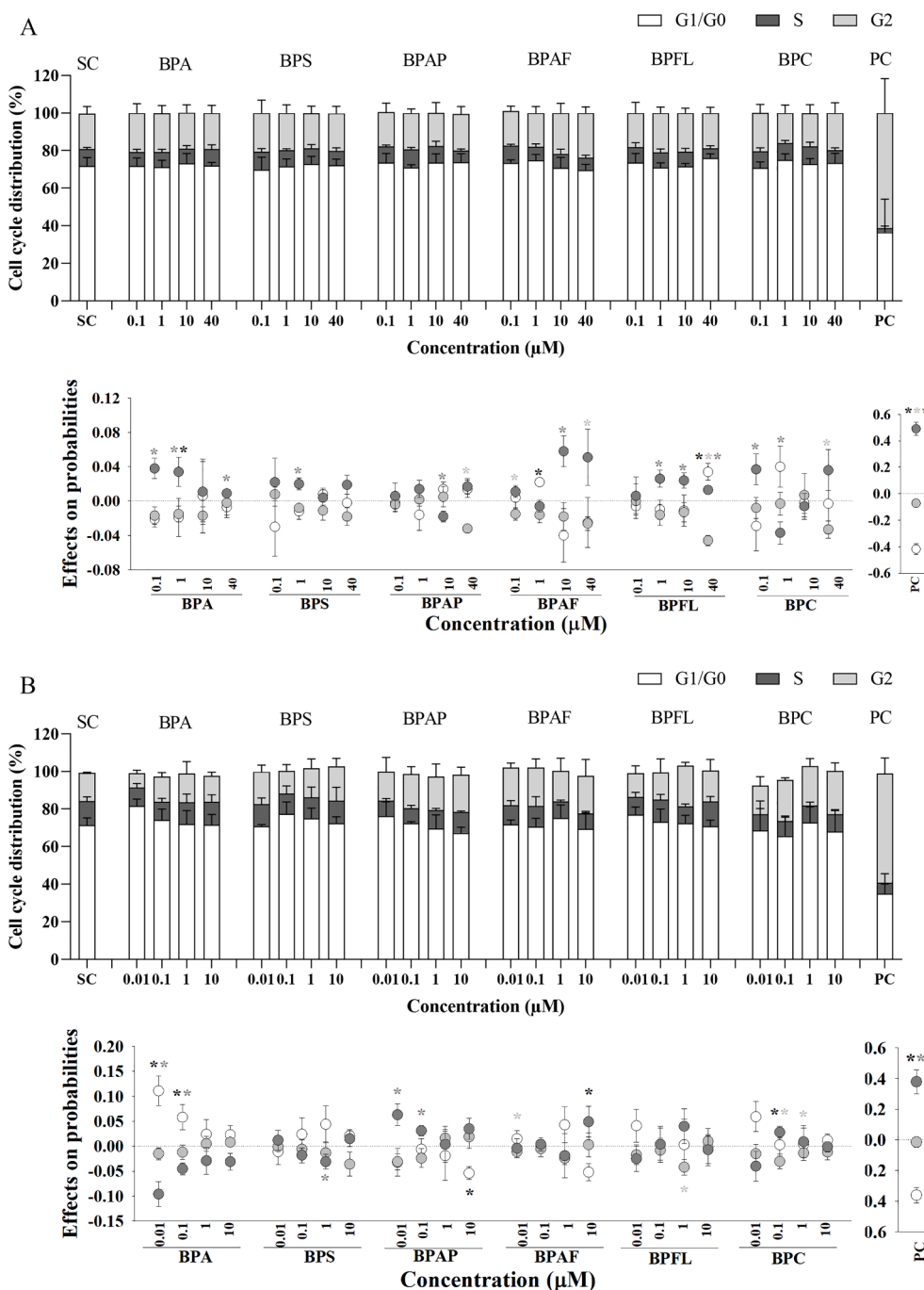
Fig. 4. Distribution of HepG2 cells from spheroids across cell cycle phases after exposure to selected BPs for 24 (A) and 96-h (B) and calculated effects of predicted probabilities with 95 % CIs after 24-h (A.1) and 96 h (B.2) of exposure in respect to SC. Cells were labelled with Hoechst dye and analysed by flow cytometry. Etoposide (1.7 µM) was considered as a positive control (PC). The % of cell cycle distribution is presented as mean (N = 3) in SigmaPlot.11 and statistical analysis was performed by multinomial logistic regression in STATA15. Asterisks show significant differences for G1 (black asterisks), S (dark grey asterisks) and G2 (light grey asterisks) phases compared to the solvent control [p < 0.05 (*)].

cells, which accounted for 2 and 74 % of all cells, respectively. The percentages of necrotic and viable cells were approximately 26 and 4 %, respectively, of all cells.

3.4. The impact of BPA and its analogues on the cell cycle, cell proliferation, gamma-H2AX positive cells and mitotic cell population

The impact of BPs on the HepG2 cell cycle, cell proliferation, DNA double-strand break formation and induction of mitotic cells was studied at two time points (24 and 96-h) by simultaneous detection of fluorescent signals (the dye Hoechst 33,258 for cell cycle and antibodies, FITC, which coincides with the proliferation marker Ki67, APC, which coincides with DNA double-strand breaks and PE, which coincides with the phosphorylated-histone 3p-H3) flow cytometry. The multi-labelling approach allows the simultaneous investigation of different endpoints in the same cells of the studied cell population and is a suitable tool for determining the geno-toxic effects caused by numerous chemicals and complex mixtures (Patra et al., 2016).

3.4.1. Cell cycle analysis

Fig. 4 shows the effects of BPs on the frequency distributions of cells among the cell cycle phases compared to the solvent control and the predicted probabilities of various potential outcomes (G0/G1, S, and G2) given a set of independent variables, calculated by multinomial logistic regression, and further post-estimation tests. The predicted probabilities allow evaluation of the effects of different concentrations of compounds on cell cycle distribution. The results showed that BPAF and BPC arrested HepG2 cells in the G2 phase after 24-hour exposure of 3-day-old spheroids. The statistically significant accumulation of cells in the presence of BPAF was found to be 5.8 percentage points at 10 μM, while BPC accumulated cells in the G2 at 40 μM however, the difference was not statistically significant compared to the solvent control. On the contrary, BPFL at 40 μM marginally arrested cells in the G0/G1 phase (by 3.4 percentage points) with a concomitant decrease in the number of cells in the S phase (by 4.6 percentage points) (Fig. 4A and Table S3). BPA and BPS did not affect the distribution of HepG2 cells across cell cycle phases.

After 96-h exposure, predicted probability indicated that BPA at the lowest concentration used (0.01 and 0.1 μM) significantly increased the amount of cells in the G0/G1 phase (by 11.1 and 5.8) percentage points, respectively), whereas it reduced the amount of cells in the S (by −1.5 and 1.2) percentage points, respectively) and G2 (by −9.6 percentage points at 0.01 μM) phases compared to solvent control cells (Fig. 4B). BPAP and BPAF increased the number of cells in the G2 phase (by 3.5 and 4.9 percentage points at 10 μM, respectively), whereas they reduced the number of cells in the G1 phase (by −4.5 and −5.2 percentage points at 10 μM, respectively) compared to solvent control cells. BPS, BPFL and BPC did not affect cell distribution in the cell cycle after prolonged exposure time.

3.4.2. Cell proliferation analysis

Cell proliferation after exposure of HepG2 spheroids to BPA and its analogues was studied using the Ki67 marker (Fig. 5). The obtained results revealed that after 24-h of exposure only BPFL and BPC affected HepG2 cell proliferation. BPFL at 10 and 40 μM inhibited cell proliferation by 12.07 % and 15.36 %, respectively, compared to the solvent control, while BPC at 40 μM decreased cell proliferation by 18.5 % (Fig. 5A). A similar effect was observed after 96-h of exposure, when BPFL and BPC at 10 μM inhibited cell proliferation by 20.85 and 7.32 % respectively, compared to the solvent control (Fig. 5B). The positive control etoposide (1.7 μM) reduced cell proliferation by 29.26 and 83.85 % compared to the solvent control after 24 and 96-h of exposure, respectively.

3.4.3. DNA double-strand breaks formation

The third endpoint measured simultaneously in the same population of HepG2 cells isolated from 3-day-old spheroids exposed to BPs for 24 and 96-h was phosphorylated histone H2AX (γH2AX), which has been described as a prospective early and sensitive marker for DNA double-strand breaks (DSBs) and DNA adducts (Kopp et al., 2019). The results showed that none of the BPs studied induced a statistically significant increase of DNA DBS after 24-h of exposure, with the exception of BPA at 40 μM (Fig. 6A). In addition, after 96-h of exposure, BPA induced a statistically significant dose-dependent increase in DNA DSB at concentrations above 1 μM (Fig. 7B). After prolonged exposure, in addition to BPA, a significant increase in DNA DBS was also detected for BPAP (0.1 and 10 μM) and BPAF (10 μM) compared to the solvent control. The positive control etoposide (1.7 μM) significantly increased the number of γH2AX positive cells compared to solvent control after both exposure times.

3.4.4. Analysis of mitotic cell population

We further measured the effect of BPA and its analogues on the occurrence of mitotic cells using the phosphorylated-histone 3p-H3 antibody (Fig. 7). The results reveal that BPAF and BPC at 40 μM caused a significant increase in mitotic cells by 5.26- and 1.48-fold, respectively, at 24-h compared to the solvent control (Fig. 7A). After prolonged 96-h exposure, BPAF at 10 μM caused a significant 1.59-fold increase in mitotic cells compared to the solvent control (Fig. 7B), while BPC did not affect the occurrence of mitotic cells after prolonged exposure. There was also a significant 1.73-fold increase in p-H3 in spheroids exposed to BPA (0.1 μM) compared to the solvent control. The positive control Colchicine (0.1 μM) induced 22.87 and 1.65-fold change in mitotic cells after 24-h and 96-h, respectively, compared to the solvent control.

3.5. The induction of DNA single-strand breaks by BPA and its analogues

DNA damage induced by BPA and its analogues after 24 and 96-h exposure of 3-day-old HepG2 spheroids was assessed by the comet assay (Fig. 8A and 8B). After 24-h of exposure BPA, BPFL and BPC did not induce DNA damage at applied concentrations (up to 40 μM). On the contrary, BPS and BPAF significantly and dose-dependently increased DNA strand break formation at 10 and 40 μM, while BPAP induced DNA damage at 40 μM (Fig. 8A). After 96-h of exposure, all BPs studied statistically significantly increased DNA single-strand break formation compared to solvent control. BPA and BPC induced DNA damage at 10 μM, while BPS, BPAF and BPFL caused elevated DNA damage at 1 and 10 μM. The most potent BP was BPAP, which significantly increased DNA damage at ≥ 0.1 μM (Fig. 8B). The positive control etoposide (17 μM) induced statistically significant DNA damage at both exposure times, as expected.

4. Discussion

The harmful effects of bisphenol A (BPA) on human health have become of great concern worldwide and have led to restrictions on its use, resulting in the increasing use of bisphenol analogues in food packaging and other consumer products (e.g., personal care products). Much is known about the toxic effects of BPA (Ďurovcová et al., 2022), whereas knowledge about the toxicity of its analogues is limited, especially since most studies focus on the effects on the reproductive system, taking into account the endocrine disrupting activity of BPA (Afifah Shamhari et al., 2021; Ahsan et al., 2018; Durovcova et al., 2018; Siracusa et al., 2018; Ullah et al., 2018, 2019). Due to insufficient information, most BPA analogues are not yet regulated and included in legislation (Durovcova et al., 2018).

In this study, the cytotoxic and genotoxic activity of BPA and the following analogues BPS, BPAP, BPAF, BPFL, and BPC was investigated. Their effects on viability and proliferation, cell cycle distribution, apoptosis/necrosis, DNA damage, and mitotic cell induction were evaluated in metabolically competent HepG2 cells grown in three-
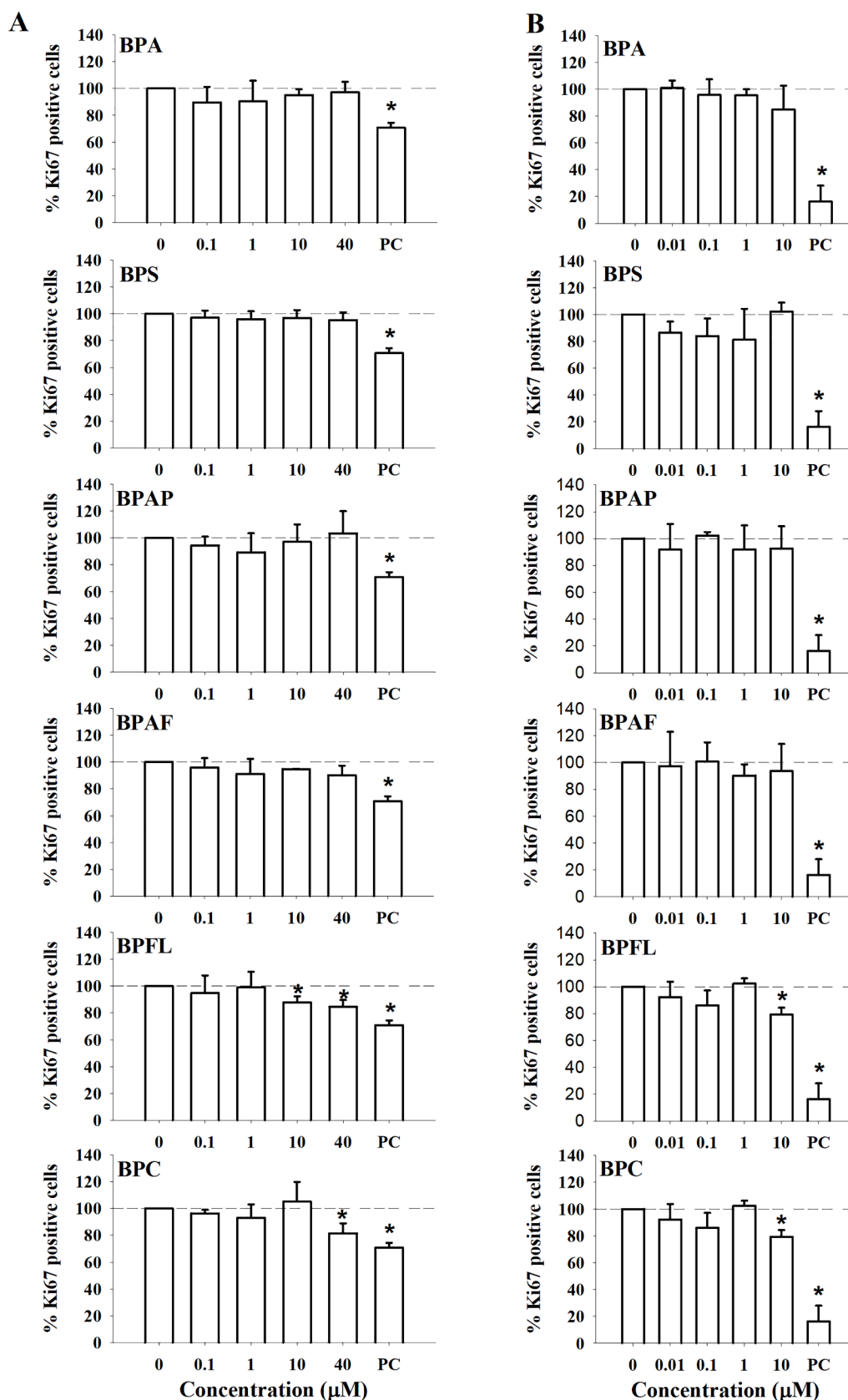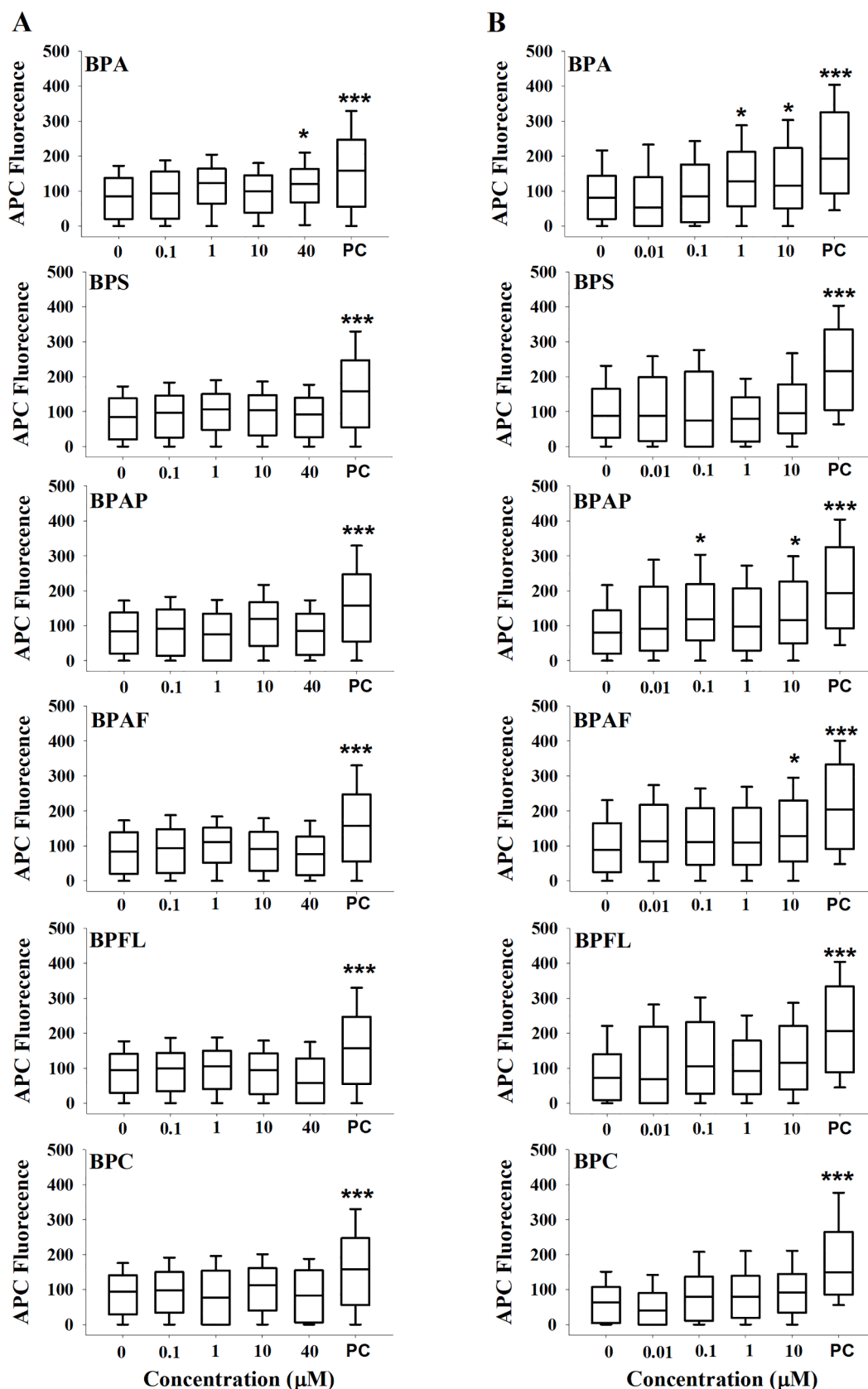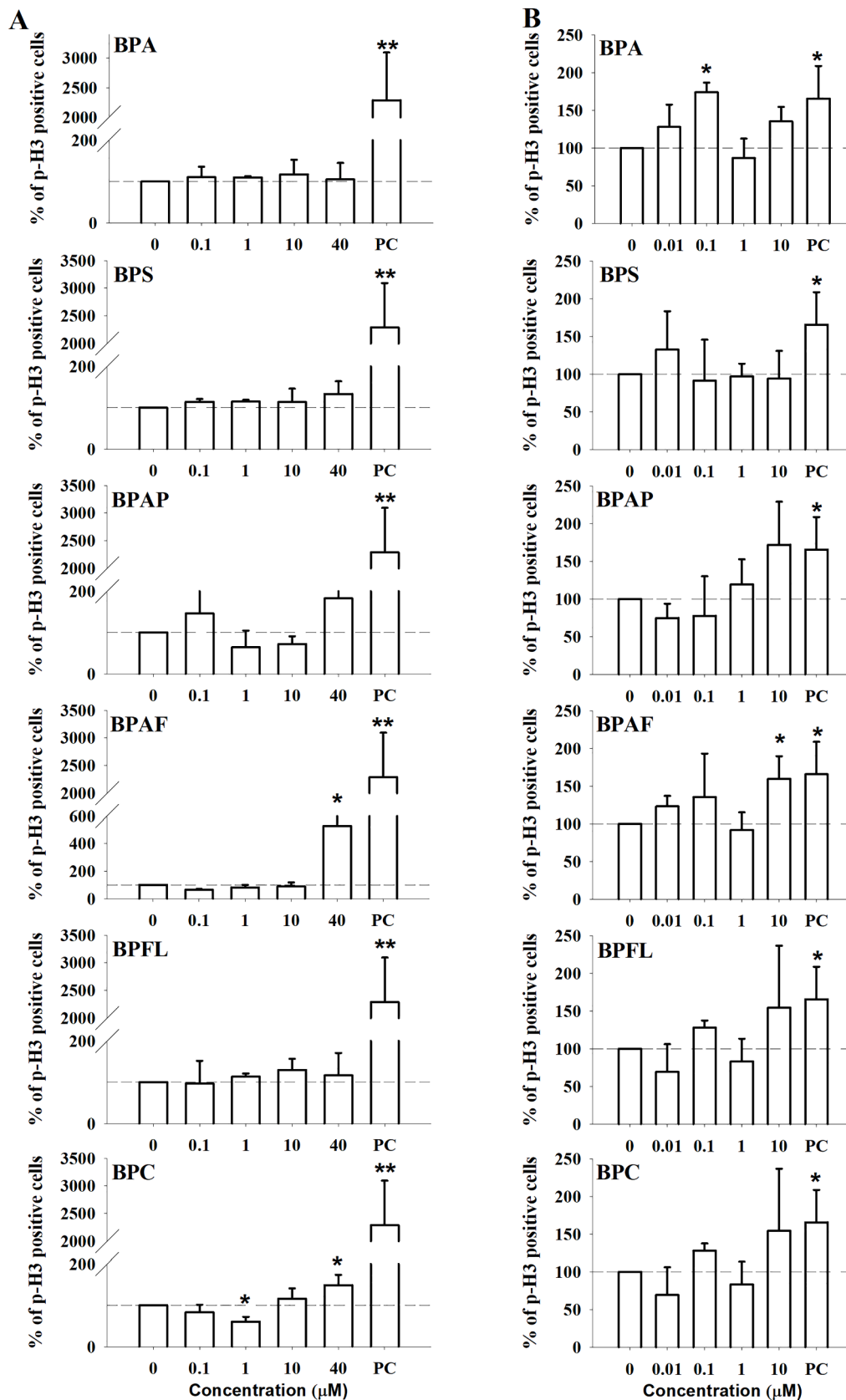
Fig. 5. Percentage of Ki67-positive cells (proliferation) compared with solvent control in HepG2 cells from spheroids after exposure to selected BPs for 24 (A) and 96-h (B) measured by flow cytometry. Etoposide (1.7 μM) served as a positive control (PC). Results are presented in bar charts as means (N = 3), and statistical analysis was performed using SigmaPlot.11 software by Two-way ANOVA with a Dunnett's post hoc test [p < 0.05 (*)].

Fig. 6. DNA double-strand breaks (assessed by γH2AX) in HepG2 cells from spheroids after exposure to selected BPs for 24 (A) and 96-h (B) using flow cytometry. Etoposide (1.7 μM) served as a positive control (PC). The distribution of data is presented in box-plots using SigmaPlot.11. Significant differences between treated samples and the solvent control (0) for γH2AX were tested using R software by the Mixed Effects Models (nlme) package by REML [p < 0.05 (*), p < 0.001 (**), p < 0.0001 (***)].

Fig. 7. Percentage of p-H3 positive cells compared with solvent control in HepG2 cells from spheroids after 24 (A) and 96-h (B) exposure to selected BPs, as measured by flow cytometry. Colchicine (0.1 μM) served as a positive control (PC). Results are presented in bar charts as means (N = 3) and statistical analysis was performed using SigmaPlot.11 software by Two-way ANOVA with a Dunnett's post hoc test [$p < 0.05$ (*), $p < 0.001$ (**)].
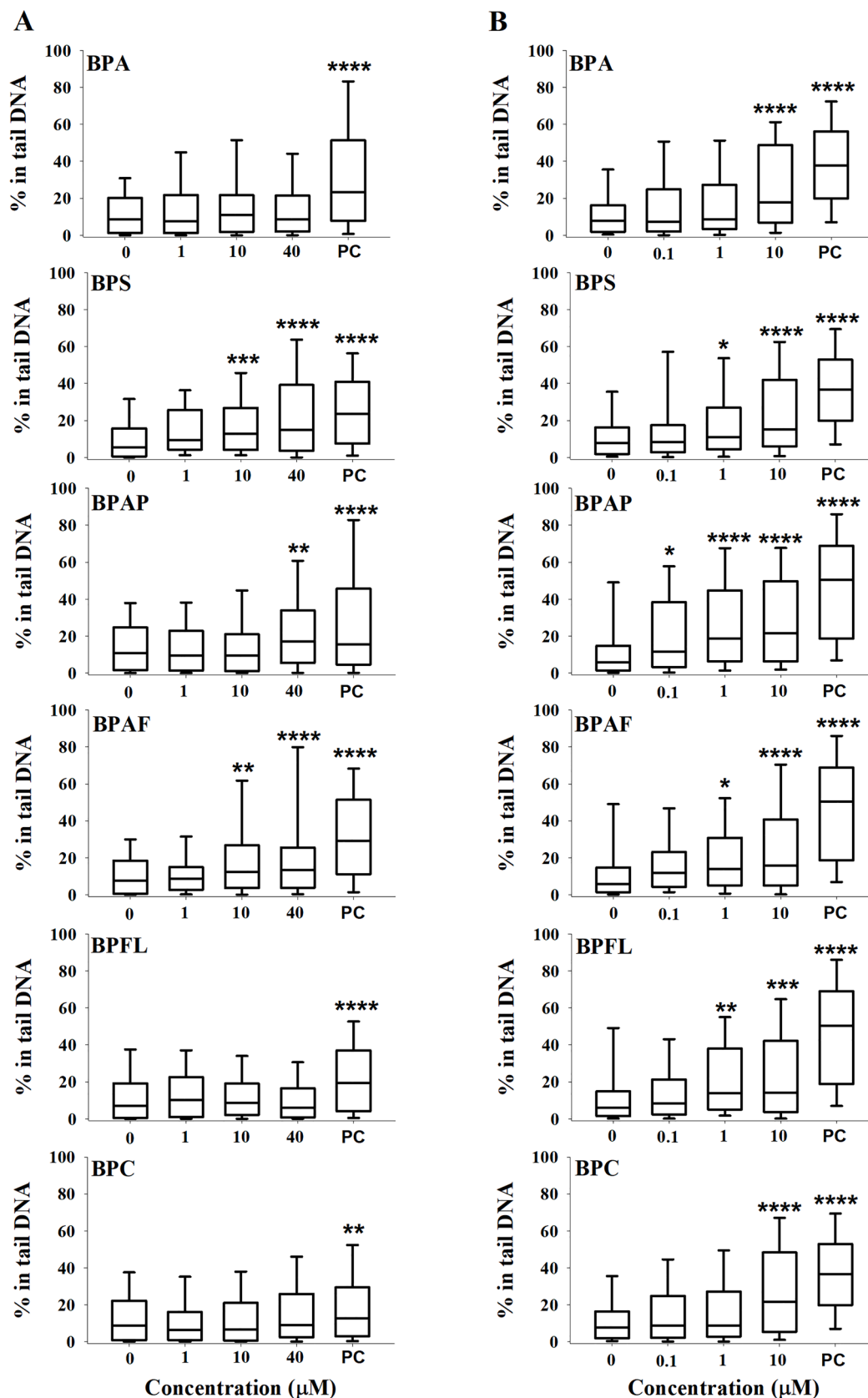
Fig. 8. DNA strand breaks in HepG2 spheroids were assessed by the comet assay after 24 (A) and 96-h (B) of exposure to selected BPs. Etoposide (17 μM) was considered as a positive control (PC). Fifty nuclei were measured per experimental point and presented in box plots using SigmaPlot.11 software. Statistical analysis was performed by two-way ANOVA [p < 0.05 (*), p < 0.001 (**), p < 0.0001 (0.0001) and p < 0.00001 (****)].

dimensional (3D) conformation. Recently, the development and use of 3D cell models, which provide more relevant information on human exposure compared to traditional two-dimensional (2D) cell models, has gained importance in toxicological studies (Elje et al., 2020; Llewellyn et al., 2020; Štampar et al., 2020). The advantage of hepatic 3D cell models is that they exhibit a higher level of liver-specific functions, including the activities of metabolic enzymes (Štampar et al., 2020), and the cell morphology and their biochemical properties are more similar to the microenvironment *in vivo*. Cells are surrounded by the natural extracellular matrix, which stimulates tissue-specific architecture and direct interactions between cells and cells with extracellular matrix (Fey and Wrzesinski, 2012; Wrzesinski and Fey, 2013). In addition, they allow for long-term repeated dose studies (Wong et al., 2011) that enable exposure to lower contaminant concentrations relevant to the environment and therefore to real human exposure scenarios.

The cytotoxicity results showed that among the BPA analogues studied, only BPFL and BPC significantly reduced HepG2 cell viability and the average surface area of HepG2 spheroids. Other BPs had no important influence on cell viability. The results are in agreement with other studies performed on HepG2 monolayer cells, where Fic et al. (Fic et al., 2013) and Hercog et al. (Hercog et al., 2019) reported that BPA and BPS had no effect on cell viability at concentrations up to 80 μM after 24-h exposure, whereas Ozyurt et al. (Ozyurt et al., 2022) reported that BPA and BPS caused a concentration-dependent decrease in HepG2 cell viability at concentrations greater than 200 μM. In contrast, Yue et al. (Yue et al., 2019), showed that a concentration of 10 μM BPA, BPAF, and BPS decreased the viability of HepG2 after 24-h of exposure. Some studies compared the cytotoxicity of BPA and its analogues in mammalian cell lines (Harnett et al., 2021; Hercog et al., 2019; Russo et al., 2018; Tsutsui et al., 2000), and the results showed that BPAF and BPC (Padberg et al., 2019) were the most toxic analogues tested. As far as we know, there is a lack of information on the cytotoxic activity of BPA analogues used in industry that contain ring systems (in the carbon bridge), such as BPFL and BPAP, or substitute the phenol ring with another functional group, such as BPC. In a study on human breast cancer cells (MDA-kb2), Ma et al. (Ma et al., 2022) investigated the toxicity of 18 BPA analogues and showed that BPFL had the greatest effect on reducing cell viability (IC50: 1.32 μM) after 24-h of exposure compared to BPA (IC50 $> 10^{-4}$ M). Our study showed that BPs affected the roundness, size, shape, compactness, surface area, and integrity of HepG2 spheroids during 96-h of exposure. BPA and BPS induced changes at 160 μM, whereas for BPAP, BPFL, BPAF, and BPC changes were observed at $\geq$ 40 μM. In addition, the exposed spheroids were less compact compared to the control spheroids as the cells loosened and detached at the surface. To our knowledge, there are few studies investigating the effects of BPA and its analogues on growth, compactness, and surface area (Park et al., 2022; Sauer et al., 2017; Xie et al., 2020), but none have been performed in 3D cell models of HepG2 cells. Previously, BPA was reported to induce morphological changes in Syrian hamster embryo (SHE) cells (Tsutsui et al., 1998), and epithelial cells isolated from the breast tissue (MCF7) (Kanai et al., 2001) cultured in a monolayer.

We further investigated the effects of selected BPs on proliferation and cell cycle distribution within the same cell population of HepG2 spheroids by flow cytometry. The Ki67 protein is a suitable marker for estimating the so-called growth fraction of a defined cell population (Scholzen and Gerdes, 2000). The results showed a decrease in Ki67-positive HepG2 cells of spheroids exposed to BPFL and BPC, while the other BPs studied did not affect HepG2 cell proliferation in a statistically significant manner. A slight reduction in cell proliferation was observed in cells exposed to BPA after prolonged exposure, but it was not statistically significant. This is consistent with previously published studies (Atlas and Dimitrova, 2019; Pfeifer et al., 2015), which reported that BPA and BPS did not significantly affect cell proliferation after prolonged exposure to low concentrations (10 μM) in human mammary epithelial cells (MCF-12A). In contrast, a BPA-mediated increase in cell

proliferation was detected in monolayer HepG2 cells when exposed to a low BPA (0.05 μM) concentration in the presence of high glucose for 48 h (Lama et al., 2019), as well as in MCF7 cells due to activation of the estrogen receptor (ER) (Potratz et al., 2017). On the contrary, a BPA-mediated decrease in cell proliferation was observed in HepG2 (Padberg et al., 2019) cells and murine osteosarcoma cells (LM8) (Kidani et al., 2017), however, these studies used higher BPA concentrations ($>$100 μM) compared to those tested in the present study. Moreover, BPA, BPS, and BPC at 100 μM decreased the proliferation of HepG2 cells (Padberg et al., 2019). BPC caused the greatest decrease, which is consistent with our results on 3D spheroids, where we showed that BPC and BPFL decreased cell proliferation even at lower concentrations (10 μM). Furthermore, Fan et al. (Fan et al., 2021), showed a decrease in cell proliferation of spheroids derived from human endometrial epithelial cells (Ishikawa cells) after exposure to 100 μM BPA, BPS and BPF, with BPA causing the greatest decrease in cell proliferation, again confirming our observation that BPA has a stronger effect than BPS.

In proliferating eukaryotic cells, the cell cycle consists of four phases, namely G1, S, G2, and M, and is regulated at several checkpoints, G1/S and G2/M being the most important ones, where decisions related to DNA replication and the completion of cell division are taken (Bartek and Lukas, 2001). When DNA damage occurs, the cell cycle is arrested until the damage is repaired, resulting in the accumulation of cells at one of the checkpoints. If DNA damage cannot be repaired, cells become apoptotic (Andrew Murray and Hunt, 1994) or mutations may occur (Lodish et al., 2000). In HepG2 cells from exposed spheroids, BPs did not have a biologically important effect on the cell cycle, however, the most severe and significant changes in cell cycle distribution were found for BPFL, where cells were arrested in the G0/G1 phase after 24-h of exposure. This may be related to the decrease in cell proliferation. It is known that decreased cell proliferation leads to increased arrest of cells in G0/G1 phase as Ki67 protein is degraded from mitosis to the G1 phase (Sobecki et al., 2017). Previously, Kidani et al. (Kidani et al., 2017) reported that BPA inhibited DNA synthesis by arresting mouse osteosarcoma (LM8) cells in G0/G1 phase and inhibited cell proliferation without affecting cell viability. Moreover, low concentrations of BPA (50 nM) time-dependently arrested human peripheral blood mononuclear (PBMC) cells in the S-phase of the cell cycle, while a high dose of BPA (100 μM) caused a significant increase in the proportion of cells in the G0/G1 phase (Di Pietro et al., 2020).

Apoptosis, or programmed cell death, is a genetically organised process that occurs when signals for survival and proliferation cease or when a cell suffers DNA damage (Ashkenazi and Salvesen, 2014); however, it is important to note that apoptosis is indicative of cell stress or cytotoxicity and not of genotoxicity (Cheung et al., 2015). Cells undergoing apoptosis disintegrate into apoptotic bodies or membrane-bound vesicles that are taken up by neighbouring cells and phagocytes. In contrast, necrosis is characterised by swelling of the cell and mitochondria and rupture of the cell membrane with the release of inflammatory cell contents into the surrounding microenvironment (Ashkenazi and Salvesen, 2014). The present study showed that BPS, BPAP, BPAF, BPFL, and BPC induced a higher percentage of apoptotic cells compared with BPA at appropriate concentrations after 24-h, whereas for BPA the highest percentage of viable cells was found among all BPs studied. A similar observation was noted after 96-h, where BPA induced the least effect on apoptotic and necrotic cell death with the highest percentage of viable cells among all BPs. Several published studies revealed that BPA exerted toxicity in a broad range of tissue cells by promoting oxidative stress and accelerating cell apoptosis, however, the underlying mechanisms are unclear (Amjad et al., 2020; Ho et al., 2017; Michałowicz et al., 2015; Ozyurt et al., 2022; Park et al., 2022; Stossi et al., 2016). Recently, Abdulhameed et al. (Abdulhameed et al., 2022) discussed in a review possible mechanisms of BPA concerning apoptosis induced in liver cells. On the other hand, there are limited literature data on apoptosis induction by other BPA analogues, which were included in the present study. Previously, Padberg et al.

(Padberg et al., 2019) reported that BPC induced to the release of cytochrome *c* from mitochondria in monolayer cultures of HepG2 cells, suggesting that BPC can induce apoptosis, whereas in the same study BPA and BPS did not affect mitochondrial membrane potential (Padberg et al., 2019).

The effect of bisphenols on DNA damage formation in HepG2 spheroids was investigated using the comet and γH2AX assays. The alkaline comet assay detects a range of DNA lesions, among them DNA SSBs and DSBs, alkali-labile sites (e.g apurinic/apyrimidinic sites), and SSBs arising from incomplete excision repair (Møller et al., 2020). On the other hand, histone H2AX is involved in maintaining genomic stability by playing a part in the DNA damage response (DDR) repair pathway to recognise and repair damaged DNA (Rahmanian et al., 2021). Phosphorylation of H2AX at serine 139 is therefore triggered by specifically DNA double-strand breaks (DSBs), resulting in γH2AX, which is known to be a sensitive marker for DNA DSBs and is a marker of clastogenicity (Cheung et al., 2015; Rogakou et al., 1998. Of the six bisphenols tested, BPS, BPAF, and BPAP exhibited stronger genotoxic potential after 24-h exposure than BPA, BPFL, and BPC, which did not induce increased DNA single-strand break (SSB) formation. At applied conditions, only BPA induced DNA DSBs. After 96-h exposure, all BPs studied statistically significantly increased DNA SSB formation detected with the comet assay, with BPAP being the most potent with an increase in DNA damage at ≥ 1 μM. BPA, BPAP, and BPAF increased the number of H2AX-positive cells, with BPAP again having the strongest effect with a LOEC of 0.1 μM. In the literature, we found only one paper describing the induction of γH2AX by submicromolar (100 nM) concentrations of BPA in HepG2 spheroids (Kim, 2018). In monolayer cultures of HepG2 cells, BPA (Hercog et al., 2019; Li et al., 2017; Ozyurt et al., 2022; Fic et al., 2013), BPAF (Hercog et al., 2019; Li et al., 2017; Fic et al., 2013), and BPS (Li et al., 2017; Ozyurt et al., 2022; Fic et al., 2013) were reported to significantly increase the frequency of DNA SSB, with BPAF being the most potent analogue. Moreover, BPA induced concentration-dependent formation of DNA DSBs in Chinese hamster (V79) cells, whereas BPS was only marginally active. In V79 cell lines expressing various human CYP enzymes (V79-hCYP1A1 cells), both BPs induced DNA strand breaks in a concentration-dependent manner (Yu et al., 2020). A greater DNA-damaging effect of BPAF compared with BPA was shown for MCF-7 cells (Lei et al., 2019). Moreover, BPAF induced DNA DSB in HepG2 cells, which are genetically engineered for expression of human CYP1A1 (HepG2-hCYP1A1) (Yang et al., 2022). Furthermore, the genotoxic activity of BPA, BPS, and BPAF was compared in human PBMC, where the results reported that BPAF was the most and BPS the least potent of the studied analogues (Mokra et al., 2015, 2017, 2018) all of them inducing oxidative DNA damage (Mokra et al., 2018). A similar observation was reported for BPA in human lymphocytes (Durovcova et al., 2018). The fact that BPA can trigger oxidative stress has been proven in numerous studies (Ďurovcová et al., 2022). Previously, increased frequency of γH2AX foci induced by BPA was reported in HepG2 (Hercog et al., 2019; Yuan et al., 2021), HepaRG (Quesnot et al., 2016), human peripheral blood mononuclear cells (Di Pietro et al., 2020), MCF-7, human bronchial epithelial (BEAS-2B) cells (George and Rupasinghe, 2018) and to lower extent also in human breast adenocarcinoma (MDA-MB-231) cells (Iso et al., 2006). Conversely, Audebert et al. (Audebert et al., 2011) described that BPA at concentrations up to 100 μM did not increase the formation of γ-H2AX foci in HepG2 cells and human epithelial colorectal adenocarcinoma cells (LS174T), it only induced a weak γH2AX signal in human renal cell adenocarcinoma cells (ACHN) at cytotoxic concentrations (50 and 100 μM). Ibuki et al. (Ibuki et al., 2008) also observed no genotoxic effects of BPA in human keratinocytes and skin fibroblasts. To the best of our knowledge, we have not found any data in the literature on the genotoxic effects of BPFL, BPAP, and BPC.

To further investigate the mode of action of BPA and its analogues, we evaluated the effects of BPs on the occurrence of mitotic cell populations by detecting phosphorylated-histone 3 (p-H3), a marker of aneugenicity (Bryce et al., 2014; Cheung et al., 2015; Muehlbauer and Schuler, 2005). Our results showed that BPAF and BPC induced phospho-histone p-H3-positive events after a 24-h exposure, with BPAF being more effective. After prolonged exposure, BPAF marginally increased p-H3-positive cells. In addition to BPAF, BPA also increased the frequency of p-H3-positive cells compared with control, but only at a low concentration (0.1 μM). The combination of γH2AX/phospho-histone p-H3 assays, allows us to distinguish whether a compound is clastogenic or aneugenic, which is not possible using the *in vitro* micronucleus assay (Bryce, 2014) unless CREST antibodies or FISH probes are used Hall et al., 2022. The results on HepG2 spheroids suggest that BPAF, which induced γH2AX and histone p-H3 positive events, acted as an aneugenic agent, whereas for BPC and BPA there is an indication that they may have an aneugenic effect, but this should be further confirmed. Previously, Yu et al. (Yu et al., 2020) described that BPA and BPS at concentrations ≥ 40 μM enhanced micronuclei formation (MN) in V79-hCYP1A1 and in a human hepatocellular carcinoma (C3A) (metabolism-proficient) cell lines. Similarly, BPAF (≥5 μM), was also reported to induce MN in C3A cells (Mokra et al., 2018; Yang et al., 2022). Moreover, in the same study, BPAF induced centromere-free micronuclei in HepG2-hCYP1A1 cells, suggesting its clastogenic activity (Mokra et al., 2018; Yang et al., 2022).

5. Conclusion

In this study, the toxic effects of BPA and its analogues (BPS, BPAP, BPAF, BPFL, and BPC) were investigated in a three-dimensional (3D) *in vitro* HepG2 cell model. The results showed for the first time that BPFL and BPC exhibited the highest cytotoxic activity among the BPA analogues tested by affecting cell viability and morphology, decreasing spheroid surface area and cell proliferation, and inducing apoptotic cell death. When the genotoxic activity was tested, the results showed that BPA, BPAP, and BPAF increased the amount of DNA double-strand breaks, indicating their clastogenic activity, while BPAF and BPC increased the frequency of p-H3-positive cells, indicating their aneugenic activity. All BPs included in the study induced DNA single-strand breaks (BPAP > BPFL > BPAF ≈ BPS > BPC ≈ BPA), with BPAP (≥0.1 μM) being the most effective and BPA and BPC being the least effective (≥1 μM) under the conditions applied. The results showed concentration- and time-dependent effects, indicating the problem of long-term and repeated exposure of humans and animals to BPA and its analogues, in which delayed effects may occur. Overall, the present results indicate that the BPA analogues BPAP, BPAF, BFL, BPS, and BPC cannot be considered safer alternatives to BPA in terms of their cytotoxic and genotoxic activities, and therefore further studies on their potential adverse effects and mechanisms of action are needed to adequately evaluate the risks of BPA analogues and assess their safety to humans.

CRediT authorship contribution statement

Declaration of Competing Interest

The authors declare that they have no known competing financial interests or personal relationships that could have appeared to influence

the work reported in this paper.

Data availability

Data will be made available on request.

Associated content

The Supporting Information is available free of charge. List of used chemicals, data showing the impact on the growth of spheroids, determination of cell death in HepG2 cells from spheroids and data showing the distribution of cells across the phases of the cell cycle.

Ethics approval.

The authors declare no involvement of Human Participants and/or Animals. In the study human cell line was used, HepG2 cells (HB-8065™) obtained by the ATCC-Cell bank.

Availability of data and material.

The authors confirm that the data supporting the findings of this study are available within the article [and/or] its supplementary materials. Generated raw data of this study are available from the corresponding author [BŽ] on request.

Appendix A. Supplementary data

Supplementary data to this article can be found online at https://doi.org/10.1016/j.envint.2022.107721.

References

Abdulhameed, A.S.A.R., Lim, V., Bahari, H., Khoo, B.Y., Abdullah, M.N.H., Tan, J.J., Yong, Y.K., 2022. Adverse Effects of Bisphenol A on the Liver and Its Underlying Mechanisms: Evidence from In Vivo and In Vitro Studies. Biomed Res. Int. 2022, 8227314. https://doi.org/10.1155/2022/8227314.

Afifah Shamhari, A., Hamid, Z.A., Budin, S.B., Shamsudin, N.J., Taib, I.S., 2021. Bisphenol a and its analogues deteriorate the hormones physiological function of the male reproductive system: A mini-review. Biomedicines 9. https://doi.org/10.3390/biomedicines9111744.

Ahsan, N., Ullah, H., Ullah, W., Jahan, S., 2018. Comparative effects of Bisphenol S and Bisphenol A on the development of female reproductive system in rats; a neonatal exposure study. Chemosphere. 197, 336–343. https://doi.org/10.1016/j.chemosphere.2017.12.118.

Amjad, S., Rahman, M.S., Pang, M.G., 2020. Role of antioxidants in alleviating bisphenol a toxicity. Biomolecules. 10, 1–26. https://doi.org/10.3390/biom10081105.

Andrew Murray, W.H., Hunt, T., 1994. The cell cycle: An introduction. Mol. Reprod. Dev. 39 https://doi.org/10.1002/mrd.1080390223.

Ashkenazi, A., Salvesen, G., 2014. Regulated cell death: signaling and mechanisms. Annu. Rev. Cell Dev. Biol. 30, 337–356. https://doi.org/10.1146/annurev-cellbio-100913-013226.

Atlas, E., Dimitrova, V., 2019. Bisphenol S and Bisphenol A disrupt morphogenesis of MCF-12A human mammary epithelial cells. Sci. Rep. 9, 1–10. https://doi.org/10.1038/s41598-019-52505-x.

Audebert, M., Dolo, L., Perdu, E., Cravedi, J.P., Zalko, D., 2011. Use of the γh2AX assay for assessing the genotoxicity of bisphenol A and bisphenol F in human cell lines. Arch. Toxicol. 85, 1463–1473. https://doi.org/10.1007/s00204-011-0721-2.

Ballesteros-Gómez, A., Brandsma, S.H., de Boer, J., Leonards, P.E.G., 2014. Analysis of two alternative organophosphorus flame retardants in electronic and plastic consumer products: Resorcinol bis-(diphenylphosphate) (PBDPP) and bisphenol A bis (diphenylphosphate) (BPA-BDPP). Chemosphere. 116, 10–14. https://doi.org/10.1016/j.chemosphere.2013.12.099.

Bartek, J., Lukas, J., 2001. Mammalian G1- and S-phase checkpoints in response to DNA damage. Curr. Opin. Cell Biol. 13, 738–747. https://doi.org/10.1016/S0955-0674(00)00280-5.

Bell, C.C., Hendriks, D.F.G., Moro, S.M.L., Ellis, E., Walsh, J., Renblom, A., Fredriksson Puigvert, L., Dankers, A.C.A., Jacobs, F., Snoeys, J., Sison-Young, R.L., Jenkins, R.E., Nordling, Å., Mkrtchian, S., Park, B.K., Kitteringham, N.R., Goldring, C.E.P., Lauschke, V.M., Ingelman-Sundberg, M., 2016. Characterization of primary human hepatocyte spheroids as a model system for drug-induced liver injury, liver function and disease. Sci. Rep. 6 https://doi.org/10.1038/srep25187.

Bokhari, M., Carnachan, R.J., Cameron, N.R., Przyborski, S.A., 2007. Culture of HepG2 liver cells on three dimensional polystyrene scaffolds enhances cell structure and function during toxicological challenge. J. Anat. 211, 567–576. https://doi.org/10.1111/j.1469-7580.2007.00778.x.

Bryce, S.D., Bemis, S.M., Mereness, J.C., Spellman, J.A., Moss, R.A., Dickinson, J., Dertinger, D., 2014. Interpreting in vitro micronucleus positive results: simple biomarker matrix discriminates clastogens, aneugens, and misleading positive agents. Environ. Mol. Mutagen. 55 (7), 542–555.

Caballero-Casero, N., Lunar, L., Rubio, S., 2016. Analytical methods for the determination of mixtures of bisphenols and derivatives in human and environmental exposure sources and biological fluids. A review. Anal. Chim. Acta. 908, 22–53. https://doi.org/10.1016/j.aca.2015.12.034.

Cantonwine, D.E., Hauser, R., Meeker, J.D., 2013. Bisphenol A and human reproductive health, Expert Rev. Obstet. Gynecol. 8, 329–335. https://doi.org/10.1586/17474108.2013.811939.

Chen, D., Kannan, K., Tan, H., Zheng, Z., Feng, Y.L., Wu, Y., Widelka, M., 2016. Bisphenol Analogues Other Than BPA: Environmental Occurrence, Human Exposure, and Toxicity - A Review. Environ. Sci. Technol. 50, 5438–5453. https://doi.org/10.1021/acs.est.5b05387.

Chen, Y., Meng, X., Zhu, Y., Shen, M., Lu, Y., Cheng, J., Xu, Y., 2018. Rapid detection of four mycotoxins in corn using a microfluidics and microarray-based immunoassay system. Talanta. 186, 299–305. https://doi.org/10.1016/j.talanta.2018.04.064.

Cheung, J.R., Dickinson, D.A., Moss, J., Schuler, M.J., Spellman, R.A., Heard, P.L., 2015. Histone markers identify the mode of action for compounds positive in the TK6 micronucleus assay. Mutat. Res. - Genet. Toxicol. Environ. Mutagen. 777, 7–16. https://doi.org/10.1016/j.mrgentox.2014.11.002.

Choi, Y.J., Lee, L.S., 2017. Partitioning Behavior of Bisphenol Alternatives BPS and BPAF Compared to BPA. Environ. Sci. Technol. 51, 3725–3732. https://doi.org/10.1021/acs.est.6b05902.

Commission, T.H.E.E., 2018. Regulation (EU) 2018/213. Off. J. Eur. Union. 2018, 6–12.

Conway, G.E., Shah, U.K., Llewellyn, S., Cervena, T., Evans, S.J., Al Ali, A.S., Jenkins, G.J., Clift, M.J.D., Doak, S.H., 2020. Adaptation of the in vitro micronucleus assay for genotoxicity testing using 3D liver models supporting longer-term exposure durations. Mutagenesis. 35, 319–330. https://doi.org/10.1093/mutage/geaa018.

Coors, A., Jones, P.D., Giesy, J.P., Ratte, H.T., 2003. Removal of estrogenic activity from municipal waste landfill leachate assessed with a bioassay based on reporter gene expression. Environ. Sci. Technol. 37, 3430–3434. https://doi.org/10.1021/es0300158.

Dai, Z., Li, Y., Yang, S., Zhao, N., Zhang, X., Xu, J., 2009. Kinetics and thermal properties of epoxy resins based on bisphenol fluorene structure. Eur. Polym. J. 45, 1941–1948. https://doi.org/10.1016/j.eurpolymj.2009.04.012.

den Braver-Sewradj, S.P., van Spronsen, R., Hessel, E.V.S., 2020. Substitution of bisphenol A: a review of the carcinogenicity, reproductive toxicity, and endocrine disruption potential of alternative substances. Crit. Rev. Toxicol. 50, 128–147. https://doi.org/10.1080/10408444.2019.1701986.

Di Pietro, P., D'Auria, R., Viggiano, A., Ciaglia, E., Meccariello, R., Dello Russo, R., Puca, A.A., Vecchione, C., Nori, S.L., Santoro, A., 2020. Bisphenol A induces DNA damage in cells exerting immune surveillance functions at peripheral and central level. Chemosphere. 254, 126819 https://doi.org/10.1016/j.chemosphere.2020.126819.

Ďurovcová, I., Kyzek, S., Fabová, J., Makuková, J., Gálová, E., Ševčovičová, A., 2022. Genotoxic potential of bisphenol A: A review. Environ. Pollut. 306 https://doi.org/10.1016/j.envpol.2022.119346.

Durovcova, I., Spackova, J., Puskar, M., Galova, E., Sevcovicova, A., 2018. Bisphenol a as an environmental pollutant with dual genotoxic and DNA-protective effects. Neuroendocrinol. Lett. 39, 294–298.

ECHA, 4,4'-[2,2,2-trifluoro-1-(trifluoromethyl)ethylidene]diphenol; Bisphenol AF European Chemicals Agency, Helsinki, Finland (2019), 2019.

ECHA, 4,4'-isopropylidenedi-o-cresol European Chemicals Agency, Helsinki, Finland (2021), 2021.

ECHA, 4, 4'-methylenediphenol European Chemicals Agency, Helsinki, Finland (2020), 2020.

Eilenberger, C., Rothbauer, M., Ehmoser, E.K., Ertl, P., Küpcü, S., 2019. Effect of Spheroidal Age on Sorafenib Diffusivity and Toxicity in a 3D HepG2 Spheroid Model. Sci. Rep. 9 https://doi.org/10.1038/s41598-019-41273-3.

Elje, E., Hesler, M., Rundén-Pran, E., Mann, P., Mariussen, E., Wagner, S., Dusinska, M., Kohl, Y., 2019. The comet assay applied to HepG2 liver spheroids. Mutat. Res. Toxicol. Environ. Mutagen. https://doi.org/10.1016/J.MRGENTOX.2019.03.006.

Elje, E., Mariussen, E., Moriones, O.H., Bastús, N.G., Puntes, V., Kohl, Y., Dusinska, M., Rundén-Pran, E., 2020. Hepato(Geno)toxicity assessment of nanoparticles in a hepg2 liver spheroid model. Nanomaterials 10. https://doi.org/10.3390/nano10030545.

Emanuelsson, I., Norlin, M., 2012. Protective effects of 27- and 24-hydroxycholesterol against staurosporine-induced cell death in undifferentiated neuroblastoma SH-SY5Y cells. Neurosci. Lett. 525, 44–48. https://doi.org/10.1016/j.neulet.2012.07.057.

EU, REGULATION (EC) No 1907/2006 OF THE EUROPEAN PARLIAMENT AND OF THE COUNCIL, 2006.

European Food Safety Authority, Scientific opinion on bisphenol A (2015), Eur. Food Saf. Auth. (2015) 4.

Fan, H., Fernando, S.R., Jiang, L., Wang, Z., Kodithuwakku, S.P., Wong, C.K.C., Ng, E.H. Y., Yeung, W.S.B., Lee, K., 2021. Bisphenol A Analogues Suppress Spheroid Attachment on Human Endometrial Epithelial Cells through Modulation of Steroid Hormone Receptors Signaling Pathway, (2021).

FDA, U.S., 2014. No Bisphenol A (BPA): Use in Food Contact Application, Public Heal. Focus. 1–8.

Fey, S.J., Wrzesinski, K., 2012. Determination of drug toxicity using 3D spheroids constructed from an immortal human hepatocyte cell line. Toxicol. Sci. 127, 403–411. https://doi.org/10.1093/toxsci/kfs122.

A. Fic, B. Žegura, M. Sollner Dolenc, M. Filipič, L.P. Mašič, MUTAGENICITY AND DNA DAMAGE OF BISPHENOL A AND ITS STRUCTURAL ANALOGUES IN HEPG2 CELLS, CELLS Arh Hig Rada Toksikol. 64 (2013) 189–200. 10.2478/10004-1254-64-2013-2319.

George, V.C., Rupasinghe, H.P.V., 2018. DNA damaging and apoptotic potentials of Bisphenol A and Bisphenol S in human bronchial epithelial cells. Environ. Toxicol. Pharmacol. 60, 52–57. https://doi.org/10.1016/j.etap.2018.04.009.

Gramec Skledar, D., Peterlin Mašič, L., 2016. Bisphenol A and its analogs: Do their metabolites have endocrine activity? Environ. Toxicol. Pharmacol. 47, 182–199. https://doi.org/10.1016/J.ETAP.2016.09.014.

Hall, N.E., Tichenor, K., Bryce, S.M., Bemis, J.C., Dertinger, S.D., 2022. In vitro human cell-based aneugen molecular mechanism assay. Environ. Mol. Mutagen. 63, 151–161. https://doi.org/10.1002/em.22480.

Harnett, K.G., Chin, A., Schuh, S.M., 2021. BPA and BPA alternatives BPS, BPAF, and TMBPF, induce cytotoxicity and apoptosis in rat and human stem cells. Ecotoxicol. Environ. Saf. 216 https://doi.org/10.1016/j.ecoenv.2021.112210.

Hercog, K., Maisanaba, S., Filipič, M., Sollner-Dolenc, M., Kač, L., Žegura, B., 2019. Genotoxic activity of bisphenol A and its analogues bisphenol S, bisphenol F and bisphenol AF and their mixtures in human hepatocellular carcinoma (HepG2) cells. Sci. Total Environ. 687, 267–276. https://doi.org/10.1016/j.scitotenv.2019.05.486.

Ho, S.M., Rao, R., To, S., Schoch, E., Tarapore, P., 2017. Bisphenol A and its analogues disrupt centrosome cycle and microtubule dynamics in prostate cancer. Endocr. Relat. Cancer. 24, 83–96. https://doi.org/10.1530/ERC-16-0175.

https://echa.europa.eu/fr/search-for-chemicals?p_p_id=disssimplesearch_WAR_disssearchportlet&p_p_lifecycle=0&_disssimplesearch_WAR_disssearchportlet_searchOccurred=true&_disssimplesearch_WAR_disssearchportlet_sessionCriteriaId=dissSimpleSearchSessionParam.

Hughes, B., 2008. Industry concern over EU hepatotoxicity guidance. Nat. Rev. Drug Discov. 7 https://doi.org/10.1038/nrd2677.

Ibuki, Y., Tani, Y., Toyooka, T., 2008. UVB-exposed chlorinated bisphenol a generates phosphorylated histone H2AX in human skin cells. Chem. Res. Toxicol. 21, 1770–1776. https://doi.org/10.1021/tx800129m.

Ikhlas, S., Usman, A., Ahmad, M., 2019. In vitro study to evaluate the cytotoxicity of BPA analogues based on their oxidative and genotoxic potential using human peripheral blood cells. Toxicol. Vitr. 60, 229–236. https://doi.org/10.1016/J.TIV.2019.06.001.

Iso, T., Watanabe, T., Iwamoto, T., Shimamoto, A., Furuichi, Y., 2006. DNA damage caused by bisphenol A and estradiol through estrogenic activity. Biol. Pharm. Bull. 29, 206–210. https://doi.org/10.1248/bpb.29.206.

Jin, H., Zhu, J., Chen, Z., Hong, Y., Cai, Z., 2018. Occurrence and Partitioning of Bisphenol Analogues in Adults' Blood from China. Environ. Sci. Technol. 52, 812–820. https://doi.org/10.1021/acs.est.7b03958.

Kanai, H., Barrett, J.C., Metzler, M., Tsutsui, T., 2001. Cell-transforming activity and estrogenicity of bisphenol-A and 4 of its analogs in mammalian cells. Int. J. Cancer. 93, 20–25. https://doi.org/10.1002/ijc.1303.

Kawagoshi, Y., Fujita, Y., Kishi, I., Fukunaga, I., 2003. Estrogenic chemicals and estrogenic activity in leachate from municipal waste landfill determined by yeast two-hybrid assay. J. Environ. Monit. 5, 269–274. https://doi.org/10.1039/b210962j.

Kidani, T., Yasuda, R., Miyawaki, J., Oshima, Y., Miura, H., Masuno, H., 2017. Bisphenol a inhibits cell proliferation and reduces the motile potential of murine LM8 osteosarcoma cells. Anticancer Res. 37, 1711–1722. https://doi.org/10.21873/anticanres.11503.

Kim, J.Y., Choi, H.G., Lee, H.M., Lee, G.A., Hwang, K.A., Choi, K.C., 2017. Effects of bisphenol compounds on the growth and epithelial mesenchymal transition of MCF-7 CV human breast cancer cells. J. Biomed. Res. 31, 358–369. https://doi.org/10.7555/JBR.31.20160162.

Kim, S., im Mun, G., Choi, E., Kim, M., Jeong, J.S., Kang, K.W., Jee, S., Lim, K.M., Lee, Y. S., 2018. Submicromolar bisphenol A induces proliferation and DNA damage in human hepatocyte cell lines in vitro and in juvenile rats in vivo. Food Chem. Toxicol. 111, 125–132. https://doi.org/10.1016/j.fct.2017.11.010.

Kopp, B., Khoury, L., Audebert, M., 2019. Validation of the γH2AX biomarker for genotoxicity assessment: a review. Arch. Toxicol. 93, 2103–2114. https://doi.org/10.1007/s00204-019-02511-9.

Galloway, L.W., Lee, T.S., Burić, B.P., Steele, I., Kocur, A.M., Pandeth, A.L., Harries, A.G., 2018. Plastics additives and human health: a case study of bisphenol a (BPA), Plast. Environ. 47, 131. (2018).

Lah, T.T., Novak, M., Pena Almidon, M.A., Marinelli, O., Bašković, B.Ž., Majc, B., Mlinar, M., Bošnjak, R., Breznik, B., Zomer, R., Nabissi, M., 2021. Cannabigerol is a potential therapeutic agent in a novel combined therapy for glioblastoma. Cells. 10, 1–22. https://doi.org/10.3390/cells10020340.

Lama, S., Vanacore, D., Diano, N., Nicolucci, C., Errico, S., Dallio, M., Federico, A., Loguercio, C., Stiuso, P., 2019. Ameliorative effect of Silybin on bisphenol A induced oxidative stress, cell proliferation and steroid hormones oxidation in HepG2 cell cultures. Sci. Rep. 9, 1–10. https://doi.org/10.1038/s41598-019-40105-8.

Lei, B., Sun, S., Zhang, X., Feng, C., Xu, J., Wen, Y., Huang, Y., Wu, M., Yu, Y., 2019. Bisphenol AF exerts estrogenic activity in MCF-7 cells through activation of Erk and PI3K/Akt signals via GPER signaling pathway. Chemosphere. 220, 362–370. https://doi.org/10.1016/j.chemosphere.2018.12.122.

Li, X., Yin, P., Zhao, L., 2017. Effects of individual and combined toxicity of bisphenol A, dibutyl phthalate and cadmium on oxidative stress and genotoxicity in HepG 2 cells. Food Chem. Toxicol. 105, 73–81. https://doi.org/10.1016/j.fct.2017.03.054.

Liao, C., Kannan, K., 2013. Concentrations and profiles of bisphenol a and other bisphenol analogues in foodstuffs from the united states and their implications for human exposure. J. Agric. Food Chem. 61, 4655–4662. https://doi.org/10.1021/jf400445n.

Liao, C., Liu, F., Kannan, K., 2012. Bisphenol S, a new bisphenol analogue, in paper products and currency bills and its association with bisphenol a residues. Environ. Sci. Technol. 46, 6515–6522. https://doi.org/10.1021/es300876n.

Liu, W., Wang, J., Qiu, Q.H., Ji, L., Wang, C.Y., Zhang, M.L., 2008. Synthesis and characterisation of 9,9-bis(4-hydroxyphenyl)-fluorene catalysed by cation exchanger. Pigment Resin Technol. 37, 9–15. https://doi.org/10.1108/03699420810839657.

Liu, J., Zhang, L., Lu, G., Jiang, R., Yan, Z., Li, Y., 2021. Occurrence, toxicity and ecological risk of Bisphenol A analogues in aquatic environment – A review. Ecotoxicol. Environ. Saf. 208 https://doi.org/10.1016/j.ecoenv.2020.111481.

Llewellyn, S.V., Conway, G.E., Shah, U.K., Evans, S.J., Jenkins, G.J.S., Clift, M.J.D., Doak, S.H., 2020. Advanced 3D liver models for in vitro genotoxicity testing following long-term nanomaterial exposure. J. Vis. Exp. 2020, 1–10. https://doi.org/10.3791/61141.

Lodish, H., Berk, A., Zipursky, S.L., Matsudaira, P., Baltimore, D., Darnell, J., 2020. DNA Damage and Repair and Their Role in Carcinogenesis, (2000). https://www.ncbi.nlm.nih.gov/books/NBK21554/ (accessed December 1, 2020).

Lucarini, F., Krasniqi, T., Bailat Rosset, G., Roth, N., Hopf, N.B., Broillet, M.-C., Staedler, D., 2020. Exposure to New Emerging Bisphenols Among Young Children in Switzerland, in. Int. J. Environ. Res. Public Health, MDPI AG 4793. https://doi.org/10.3390/ijerph17134793.

Ma, M., Zhao, W., Tan, T., Hitabatuma, A., Wang, P., Wang, R., Su, X., 2022. Study of eighteen typical bisphenol analogues as agonist or antagonist for androgen and glucocorticoid at sub-micromolar concentrations in vitro. Sci. Total Environ. 822, 153439 https://doi.org/10.1016/j.scitotenv.2022.153439.

Mandon, M., Huet, S., Dubreil, E., Fessard, V., Le Hégarat, L., 2019. Three-dimensional HepaRG spheroids as a liver model to study human genotoxicity in vitro with the single cell gel electrophoresis assay. Sci. Rep. 9 https://doi.org/10.1038/s41598-019-47114-7.

Masoner, J.R., Kolpin, D.W., Furlong, E.T., Cozzarelli, I.M., Gray, J.L., Schwab, E.A., 2014. Contaminants of emerging concern in fresh leachate from landfills in the conterminous United States. Environ. Sci. Process. Impacts. 16, 2335–2354. https://doi.org/10.1039/c4em00124a.

Michałowicz, J., Mokra, K., Bak, A., 2015. Bisphenol A and its analogs induce morphological and biochemical alterations in human peripheral blood mononuclear cells (in vitro study). Toxicol. Vitr. 29, 1464–1472. https://doi.org/10.1016/j.tiv.2015.05.012.

Mokra, K., Kocia, M., Michałowicz, J., 2015. Bisphenol A and its analogs exhibit different apoptotic potential in peripheral blood mononuclear cells (in vitro study). Food Chem. Toxicol. 84, 79–88. https://doi.org/10.1016/j.fct.2015.08.007.

Mokra, K., Kuźmińska-Surowaniec, A., Woźniak, K., Michałowicz, J., 2017. Evaluation of DNA-damaging potential of bisphenol A and its selected analogs in human peripheral blood mononuclear cells (in vitro study). Food Chem. Toxicol. 100, 62–69. https://doi.org/10.1016/j.fct.2016.12.003.

Mokra, K., Woźniak, K., Bukowska, B., Sicińska, P., Michałowicz, J., 2018. Low-concentration exposure to BPA, BPF and BPAF induces oxidative DNA bases lesions in human peripheral blood mononuclear cells. Chemosphere. 201, 119–126. https://doi.org/10.1016/j.chemosphere.2018.02.166.

Møller, P., Azqueta, A., Boutet-Robinet, E., Koppen, G., Bonassi, S., Milić, M., Gajski, G., Costa, S., Teixeira, J.P., Costa Pereira, C., Dusinska, M., Godschalk, R., Brunborg, G., Gutzkow, K.B., Giovannelli, L., Cooke, M.S., Richling, E., Laffon, B., Valdiglesias, V., Basaran, N., del Bo, C., Zegura, B., Novak, M., Stopper, H., Vodicka, P., Vodenkova, S., de Andrade, V.M., Sramkova, M., Gabelova, A., Collins, A., Langie, S. A.S., 2020. Minimum Information for Reporting on the Comet Assay (MIRCA): recommendations for describing comet assay procedures and results. Nat. Protoc. 1512 (15), 3817–3826. https://doi.org/10.1038/s41596-020-0398-1.

Muehlbauer, P.A., Schuler, M.J., 2005. Detection of numerical chromosomal aberrations by flow cytometry: A novel process for identifying aneugenic agents. Mutat. Res. - Genet. Toxicol. Environ. Mutagen. 585, 156–169. https://doi.org/10.1016/j.mrgentox.2005.05.002.

Ozyurt, B., Ozkemahli, G., Yirun, A., Ozyurt, A.B., Bacanli, M., Basaran, N., Kocer-Gumusel, B., Erkekoglu, P., 2022. Comparative evaluation of the effects of bisphenol derivatives on oxidative stress parameters in HepG2 cells. Drug Chem. Toxicol. 1–9. https://doi.org/10.1080/01480545.2022.2028823.

Padberg, F., Tarnow, P., Luch, A., Zellmer, S., 2019. Minor structural modifications of bisphenol A strongly affect physiological responses of HepG2 cells. Arch. Toxicol. 93, 1529–1541. https://doi.org/10.1007/s00204-019-02457-y.

Park, C.G., Jun, I., Lee, S., Ryu, C.S., Lee, S.A., Park, J., Han, H.S., Park, H., Manz, A., Shin, H., Kim, Y.J., 2022. Integration of Bioinspired Fibrous Strands with 3D Spheroids for Environmental Hazard Monitoring. Small. 18, 1–12. https://doi.org/10.1002/smll.202200757.

Patra, B., Peng, C.C., Liao, W.H., Lee, C.H., Tung, Y.C., 2016. Drug testing and flow cytometry analysis on a large number of uniform sized tumor spheroids using a microfluidic device. Sci. Rep. 6 https://doi.org/10.1038/srep21061.

Pelch, K., Wignall, J.A., Goldstone, A.E., Ross, P.K., Blain, R.B., Shapiro, A.J., Holmgren, S.D., Hsieh, J.H., Svoboda, D., Auerbach, S.S., Parham, F.M., Masten, S. A., Walker, V., Rooney, A., Thayer, K.A., 2019. A scoping review of the health and toxicological activity of bisphenol A (BPA) structural analogues and functional alternatives. Toxicology. 424 https://doi.org/10.1016/j.tox.2019.06.006.

Pfeifer, D., Chung, Y.M., Hu, M.C.T., 2015. Effects of low-dose bisphenol A on DNA damage and proliferation of breast cells: The role of c-Myc. Environ. Health Perspect. 123, 1271–1279. https://doi.org/10.1289/ehp.1409199.

Pfuhler, S., van Benthem, J., Curren, R., Doak, S.H., Dusinska, M., Hayashi, M., Heflich, R.H., Kidd, D., Kirkland, D., Luan, Y., Ouedraogo, G., Reisinger, K., Sofuni, T., van Acker, F., Yang, Y., Corvi, R., 2020. Use of in vitro 3D tissue models in genotoxicity testing: Strategic fit, validation status and way forward. Report of the working group from the 7th International Workshop on Genotoxicity Testing (IWGT), Mutat. Res. - Genet. Toxicol. Environ. Mutagen. 850–851. 10.1016/j.mrgentox.2020.503135.

Potratz, S., Tarnow, P., Jungnickel, H., Baumann, S., Von Bergen, M., Tralau, T., Luch, A., 2017. Combination of Metabolomics with Cellular Assays Reveals New Biomarkers and Mechanistic Insights on Xenoestrogenic Exposures in MCF-7 Cells. Chem. Res. Toxicol. 30, 883–892. https://doi.org/10.1021/acs.chemrestox.6b00106.

Pradesh, M., Singh, I.R., Talpade, J., Shrman, K., Sharma, R.K., Gutham, V., Singh, R.P., Meena, N.S., 2018. Bisphenol a: An endocrine disruptor, ∼ 394 ∼. J. Entomol. Zool. Stud. 6.

Pritchett, J.J., Kuester, R.K., Sipes, I.G., 2002. Metabolism of Bisphenol A in Primary Cultured Hepatocytes from Mice, Rats, and Humans. Drug Metab. Dispos. 30, 1180–1185. https://doi.org/10.1124/DMD.30.11.1180.

Quesnot, N., Rondel, K., Audebert, M., Martinais, S., Glaise, D., Morel, F., Loyer, P., Robin, M.A., 2016. Evaluation of genotoxicity using automated detection of γH2AX in metabolically competent HepaRG cells. Mutagenesis. 31, 43–50. https://doi.org/10.1093/mutage/gev059.

Rahmanian, N., Shokrzadeh, M., Eskandani, M., 2021. Recent advances in γH2AX biomarker-based genotoxicity assays: A marker of DNA damage and repair. DNA Repair (Amst). 108 https://doi.org/10.1016/j.dnarep.2021.103243.

Ramaiahgari, S.C., Den Braver, M.W., Herpers, B., Terpstra, V., Commandeur, J.N.M., Van De Water, B., Price, L.S., 2014. A 3D in vitro model of differentiated HepG2 cell spheroids with improved liver-like properties for repeated dose high-throughput toxicity studies. Arch. Toxicol. 88, 1083–1095. https://doi.org/10.1007/s00204-014-1215-9.

Rezg, R., El-Fazaa, S., Gharbi, N., Mornagui, B., 2014. Bisphenol A and human chronic diseases: Current evidences, possible mechanisms, and future perspectives. Environ. Int. 64, 83–90. https://doi.org/10.1016/j.envint.2013.12.007.

Rochester, J.R., 2013. Bisphenol A and human health: A review of the literature. Reprod. Toxicol. 42, 132–155. https://doi.org/10.1016/j.reprotox.2013.08.008.

Rogakou, E., Pilch, D.R., Orr, A.H., Ivanova, V.S., Bonner, W.M., 1998. DNA double-stranded breaks induce histone H2AX phosphorylation on serine 139. J. Biol. Chem. 273, 5858–5868. https://doi.org/10.1074/jbc.273.10.5858.

Russo, G., Capuozzo, A., Barbato, F., Irace, C., Santamaria, R., Grumetto, L., 2018. Cytotoxicity of seven bisphenol analogues compared to bisphenol A and relationships with membrane affinity data. Chemosphere. 201, 432–440. https://doi.org/10.1016/j.chemosphere.2018.03.014.

Russo, G., Barbato, F., Mita, D.G., Grumetto, L., 2019. Occurrence of Bisphenol A and its analogues in some foodstuff marketed in Europe. Food Chem. Toxicol. 131 https://doi.org/10.1016/j.fct.2019.110575.

Sauer, S.J., Tarpley, M., Shah, I., Save, A.V., Lyerly, H.K., Patierno, S.R., Williams, K.P., Devi, G.R., 2017. Bisphenol A activates EGFR and ERK promoting proliferation, tumor spheroid formation and resistance to EGFR pathway inhibition in estrogen receptornegative inflammatory breast cancer cells. Carcinogenesis. 38, 252–260. https://doi.org/10.1093/carcin/bgx003.

Scholzen, T., Gerdes, J., 2000. The Ki-67 protein: From the known and the unknown. J. Cell. Physiol. 182, 311–322. https://doi.org/10.1002/(SICI)1097-4652(200003)182:3<311::AID-JCP1>3.0.CO;2-9.

Seachrist, D.D., Bonk, K.W., Ho, S.M., Prins, G.S., Soto, A.M., Keri, R.A., 2016. A review of the carcinogenic potential of bisphenol A. Reprod. Toxicol. 59, 167–182. https://doi.org/10.1016/j.reprotox.2015.09.006.

Sendra, B., Pereiro, M., Fuigueras, P., Novoa, A., 2020. An integrative toxicogenomic analysis of plastic additives, J. Hazard. Mater. In press.

Shah, U.K., de O. Mallia, J., Singh, N., Chapman, K.E., Doak, S.H., Jenkins, G.J.S., 2018. A three-dimensional in vitro HepG2 cells liver spheroid model for genotoxicity studies. Mutat. Res. - Genet. Toxicol. Environ. Mutagen. 825, 51–58. https://doi.org/10.1016/j.mrgentox.2017.12.005.

Shah, U.K., Verma, J.R., Chapman, K.E., Wilde, E.C., Tonkin, J.A., Brown, M.R., Johnson, G.E., Doak, S.H., Jenkins, G.J., 2020. Detection of urethane-induced genotoxicity in vitro using metabolically competent human 2D and 3D spheroid

culture models. Mutagenesis. 35, 445–452. https://doi.org/10.1093/mutage/geaa029.

Shen, Y., Ren, M.L., Feng, X., Cai, Y.L., Gao, Y.X., Xu, Q., 2014. An evidence in vitro for the influence of bisphenol A on uterine leiomyoma. Eur. J. Obstet. Gynecol. Reprod. Biol. 178, 80–83. https://doi.org/10.1016/j.ejogrb.2014.03.052.

Siracusa, J.S., Yin, L., Measel, E., Liang, S., Yu, X., 2018. Effects of bisphenol A and its analogs on reproductive health: A mini review. Reprod. Toxicol. 79, 96–123. https://doi.org/10.1016/j.reprotox.2018.06.005.

Sobecki, M., Mrouj, K., Colinge, J., Gerbe, F., Jay, P., Krasinska, L., Dulic, V., Fisher, D., 2017. Cell-cycle regulation accounts for variability in Ki-67 expression levels. Cancer Res. 77, 2722–2734. https://doi.org/10.1158/0008-5472.CAN-16-0707.

Štampar, M., Tomc, J., Filipič, M., Žegura, B., 2019. Development of in vitro 3D cell model from hepatocellular carcinoma (HepG2) cell line and its application for genotoxicity testing. Arch. Toxicol. 93, 3321–3333. https://doi.org/10.1007/s00204-019-02576-6.

Štampar, M., Frandsen, H.S., Rogowska-Wrzesinska, A., Wrzesinski, K., Filipič, M., Žegura, B., 2020. Hepatocellular carcinoma (HepG2/C3A) cell-based 3D model for genotoxicity testing of chemicals. Sci. Total Environ., 143255 https://doi.org/10.1016/j.scitotenv.2020.143255.

Štampar, M., Breznik, B., Filipič, M., Žegura, B., 2020. Characterization of In Vitro 3D Cell Model Developed from Human Hepatocellular Carcinoma (HepG2) Cell Line. Cells. 9, 2557. https://doi.org/10.3390/cells9122557.

Štampar, M., Žabkar, S., Filipič, M., Žegura, B., 2022. HepG2 spheroids as a biosensor-like cell-based system for (geno)toxicity assessment. Chemosphere. 291 https://doi.org/10.1016/J.CHEMOSPHERE.2021.132805.

Stossi, F., Dandekar, R.D., Bolt, M.J., Newberg, J.Y., Mancini, M.G., Kaushik, A.K., Putluri, V., Sreekumar, A., Mancini, M.A., 2016. High throughput microscopy identifies bisphenol AP, a bisphenol A analog, as a novel AR down-regulator, Oncotarget. 7, 16962–16974. 10.18632/oncotarget.7655.

Thomas, D., 2016. Costs, benefits, and adoption of additive manufacturing: a supply chain perspective. Int. J. Adv. Manuf. Technol. 85, 1857–1876. https://doi.org/10.1007/s00170-015-7973-6.

Tsutsui, T., Tamura, Y., Yagi, E., Hasegawa, K., Takahashi, M., Maizumi, N., Yamaguchi, F., Barrett, J.C., 1998. Bisphenol-A induces cellular transformation, aneuploidy and DNA adduct formation in cultured Syrian hamster embryo cells. Int. J. Cancer. 75, 290–294. https://doi.org/10.1002/(SICI)1097-0215(19980119)75:2<290::AID-IJC19>3.0.CO;2-H.

Tsutsui, T., Tamura, Y., Suzuki, A., Hirose, Y., Kobayashi, M., Nishimura, H., Metzler, M., Barrett, J.C., 2000. Mammalian cell transformation and aneuploidy induced by five bisphenols. Int. J. Cancer. 86, 151–154. https://doi.org/10.1002/(SICI)1097-0215(20000415)86:2<151::AID-IJC1>3.0.CO;2-0.

Ullah, A., Pirzada, M., Jahan, S., Ullah, H., Shaheen, G., Rehman, H., Siddiqui, M.F., Butt, M.A., 2018. Bisphenol A and its analogs bisphenol B, bisphenol F, and bisphenol S: Comparative in vitro and in vivo studies on the sperms and testicular tissues of rats. Chemosphere. 209, 508–516. https://doi.org/10.1016/j.chemosphere.2018.06.089.

Ullah, A., Pirzada, M., Afsar, T., Razak, S., Almajwal, A., Jahan, S., 2019. Effect of bisphenol F, an analog of bisphenol A, on the reproductive functions of male rats, Environ. Health. Prev. Med. 24, 1–11. https://doi.org/10.1186/s12199-019-0797-5.

Usman, A., Ahmad, M., 2016. From BPA to its analogues: Is it a safe journey? Chemosphere. 158, 131–142. https://doi.org/10.1016/j.chemosphere.2016.05.070.

Vandenberg, L.N., Colborn, T., Hayes, T.B., Heindel, J.J., Jacobs, D.R., Lee, D.H., Shioda, T., Soto, A.M., vom Saal, F.S., Welshons, W.V., Zoeller, R.T., Myers, J.P., 2012. Hormones and endocrine-disrupting chemicals: Low-dose effects and nonmonotonic dose responses. Endocr. Rev. 33, 378–455. https://doi.org/10.1210/er.2011-1050.

Wisniewski, P., Romano, R.M., Kizys, M.M.L., Oliveira, K.C., Kasamatsu, T., Giannocco, G., Chiamolera, M.I., Dias-da-Silva, M.R., Romano, M.A., 2015. Adult exposure to bisphenol A (BPA) in Wistar rats reduces sperm quality with disruption of the hypothalamic-pituitary-testicular axis. Toxicology. 329, 1–9. https://doi.org/10.1016/j.tox.2015.01.002.

Wong, S.F., No, D.Y., Choi, Y.Y., Kim, D.S., Chung, B.G., Lee, S.H., 2011. Concave microwell based size-controllable hepatosphere as a three-dimensional liver tissue model. Biomaterials. 32, 8087–8096. https://doi.org/10.1016/j.biomaterials.2011.07.028.

Wrzesinski, K., Fey, S.J., 2013. After trypsinisation, 3D spheroids of C3A hepatocytes need 18 days to re-establish similar levels of key physiological functions to those seen in the liver. Toxicol. Res. (Camb) 2, 123–135. https://doi.org/10.1039/c2tx20060k.

Wrzesinski, S.K., Fey, J., 2015. From 2D to 3D-a new dimension for modelling the effect of natural products on human tissue. Curr. Pharm. Des. 21 (38), 5605–5616.

Xiao, X., Li, J., Yu, T., Zhou, L., Fan, X., Xiao, H., Wang, Y., Yang, L., Lv, J., Jia, X., Zhang, Z., 2018. Bisphenol AP is anti-estrogenic and may cause adverse effects at low doses relevant to human exposure. Environ. Pollut. 242, 1625–1632. https://doi.org/10.1016/j.envpol.2018.07.115.

Xie, P., Liang, X., Song, Y., Cai, Z., 2020. Mass spectrometry imaging combined with metabolomics revealing the proliferative effect of environmental pollutants on multicellular tumor spheroids. Anal. Chem. 92, 11341–11348. https://doi.org/10.1021/acs.analchem.0c02025.

Yang, Z., Yu, H., Tu, H., Chen, Z., Hu, K., Jia, H., Liu, Y., 2022. Influence of aryl hydrocarbon receptor and sulfotransferase 1A1 on bisphenol AF-induced

clastogenesis in human hepatoma cells. Toxicology. 471, 153175 https://doi.org/10.1016/j.tox.2022.153175.

Yu, H., Chen, Z., Hu, K., Yang, Z., Song, M., Li, Z., Liu, Y., 2020. Potent Clastogenicity of Bisphenol Compounds in Mammalian Cells - Human CYP1A1 Being a Major Activating Enzyme. Environ. Sci. Technol. 54, 15267–15276. https://doi.org/10.1021/acs.est.0c04808.

Yuan, J., Che, S., Zhang, L., Li, X., Yang, J., Sun, X., Ruan, Z., 2021. Assessing the combinatorial cytotoxicity of the exogenous contamination with BDE-209, bisphenol A, and acrylamide via high-content analysis. Chemosphere. 284, 131346 https://doi.org/10.1016/j.chemosphere.2021.131346.

Yue, S., Yu, J., Kong, Y., Chen, H., Mao, M., Ji, C., Shao, S., Zhu, J., Gu, J., Zhao, M., 2019. Metabolomic modulations of HepG2 cells exposed to bisphenol analogues. Environ. Int. 129, 59–67. https://doi.org/10.1016/j.envint.2019.05.008.

Zhang, L., Fang, P., Yang, L., Zhang, J., Wang, X., 2013. Rapid method for the separation and recovery of endocrine-disrupting compound bisphenol AP from wastewater. Langmuir. 29, 3968–3975. https://doi.org/10.1021/la304792m.

Zhou, W., Fang, F., Zhu, W., Chen, Z.J., Du, Y., Zhang, J., 2017. Bisphenol A and Ovarian reserve among infertile women with polycystic Ovarian syndrome. Int. J. Environ. Res. Public Health. 14 https://doi.org/10.3390/ijerph14010018.

Zühlke, M.K., Schlüter, R., Mikolasch, A., Henning, A.K., Giersberg, M., Lalk, M., Kunze, G., Schweder, T., Urich, T., Schauer, F., 2020. Biotransformation of bisphenol A analogues by the biphenyl-degrading bacterium Cupriavidus basilensis - a structure-biotransformation relationship. Appl. Microbiol. Biotechnol. 104, 3569–3583. https://doi.org/10.1007/s00253-020-10406-4.

Further reading

Commission, E., 2001. COMMISSION REGULATION (EU) 2016/2235 of 12 December 2016 amending Annex XVII to Regulation (EC) No 1907/2006 of the European Parliament and of the Council concerning the Registration, Evaluation, Authorisation and Restriction of Chemicals (REACH) as regar. Off. J. Eur. Union. 2016, 20–30.